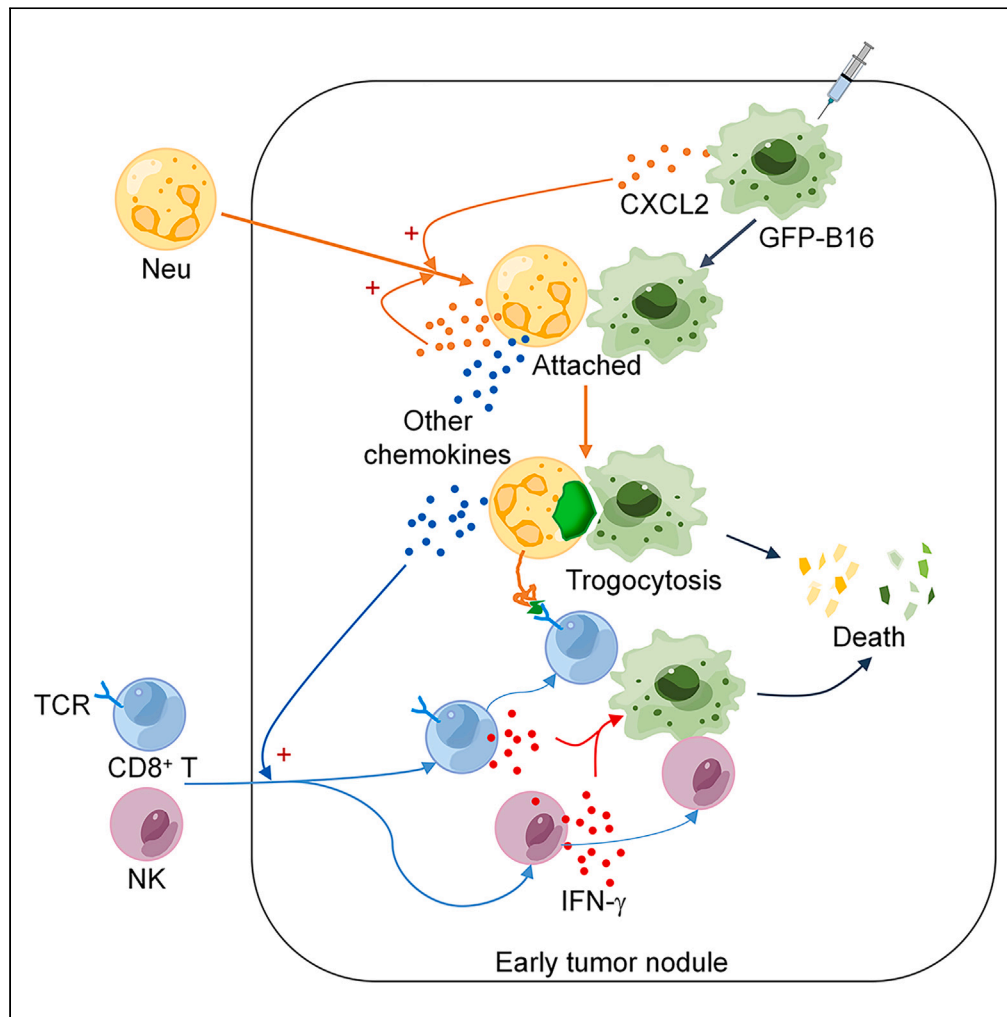**Article**

The trogocytosis of neutrophils on initial transplanted tumor in mice

Mengru Zhu,
Shengnan Wang,
Kuo Qu, ..., Yongli
Yu, Liying Wang,
Chaoying Yan

wangliy@jlu.edu.cn (L.W.)
yancy@jlu.edu.cn (C.Y.)

Highlights

Neutrophils recruited by
early tumor nodules attack
tumor cells through
trogocytosis

Increasing total or
trogocytic neutrophils
elevates nodule $CD8^+$
T/NK cells and IFN-γ

Inhibition of neutrophil
recruitment leads to the
enlargement of early tumor
nodules

Neutrophils in early tumor
nodules benefit anti-tumor
microenvironment
formation

Article

The trogocytosis of neutrophils on initial transplanted tumor in mice

Mengru Zhu,[1] Shengnan Wang,[2] Kuo Qu,[3] Feiyu Lu,[2,4] Mengyuan Kou,[3] Yunpeng Yao,[2] Tong Zhu,[1] Yongli Yu,[3] Liying Wang,[1,2,5,*] and Chaoying Yan[1,*]

SUMMARY

The role of neutrophils in tumor initiation stage is rarely reported because of the lack of suitable models. We found that neutrophils recruited in early tumor nodules induced by subcutaneous inoculation of B16 melanoma cells were able to attack tumor cells by trogocytosis. The anti-tumor immunotherapy like peritoneal injection with TLR9 agonist CpG oligodeoxynucleotide combined with transforming growth factor β2 inhibitor TIO3 could increase the trogocytic neutrophils in the nodules, as well as CD8^{+} T cells, natural killer (NK) cells, and their interferon-γ production. Local use of *Cxcl2* small interfering RNA significantly reduced the number of neutrophils and trogocytic neutrophils in tumor nodules, as well as CD8^{+} T and NK cells, and also enlarged the nodules. These results suggest that neutrophils recruited early to the inoculation site of tumor cells are conducive to the establishment of anti-tumor immune microenvironment. Our findings provide a useful model system for studying the effect of neutrophils on tumors and anti-tumor immunotherapy.

INTRODUCTION

Neutrophils are polymorphonuclear granulocytes (PMNs) that play an important role in the innate immune system. In the pathogen infection, neutrophils are the first line of defense against pathogenic microorganisms to exert an anti-infection role through a variety of their natural functions, such as degranulation, phagocytosis, and release of neutrophil extracellular traps (NETs).[1–4] In NETs, neutrophil genomic DNA contained therein has been shown to activate Toll-like receptor 9 (TLR9)-mediated immune response during inflammation.[5–8] In fact, neutrophils are also the first innate immune cells to reach the inoculation site of tumor cell transplantation at the early stage. Our previous study in subcutaneous tumor model mice found that about 90% of CD45^{+} leukocytes in tumor nodules formed at 24 h after subcutaneous tumor cell inoculation were Ly6G^{+} neutrophils.[9] It is generally believed that neutrophils are recruited to the sites of inflammation or injury for one task only of participating in the inflammatory response or repair of tissue damage,[10,11] but their role in tumors is often considered to have a dual role of pro-tumor or anti-tumor.[12,13] There has been a lot of research on neutrophils promoting tumor growth in a variety of ways, like promoting the expression of PD-L1[14] on tumor cells and inhibiting the function of CD8^{+} T cells and natural killer (NK) cells.[15,16] In an orthotopic pancreatic cancer mouse model, the presence of neutrophils was shown to be associated with functional suppression of the CD8^{+} T cells.[17] However, the ability of neutrophils to exert anti-tumor effects by assisting anti-tumor immunotherapy[18] or through their own natural properties[19–23] is more thought-provoking and intriguing. Studies have shown that neutrophils are required for the complete tumor eradication during the anti-tumor immunotherapy with melanoma-specific CD4^{+} T cells combined with OX40 co-stimulation or CTLA-4 blockade.[24] A sharp increase in the number of tumor neutrophils in lung cancer patients induced by immunotherapy is positively associated with the favorable outcome of the disease.[25] Neutrophils have also been found to impede early tumor growth and progression by various ways.[26] Research has shown that neutrophils can oppose uterine epithelial carcinogenesis via debridement of hypoxic tumor cells.[26] In the early stages of human lung cancer and several other cancers, neutrophils stimulate T cell responses by increasing antigen presentation and T cell co-stimulation.[27,28] In addition, neutrophils can also selectively kill many types of cancer cells through their natural function such as phagocytosis, releasing reactive oxygen species (ROS), elastase, and cathepsin-G.[19–21] In a mouse model of uterine adenocarcinoma, neutrophils kill tumor cells via nicotinamide adenine dinucleotide phosphate (NADPH) oxidase, ROS, and matrix metalloproteinase-9 (MMP-9), and the killing is augmented by relieving hypoxia.[29] Neutrophils promote Lewis lung carcinoma cell killing by releasing nitric oxide.[30] Adoptive transfer of neutrophils from β-glucan-trained mice to naive recipients suppressed tumor growth in an ROS-dependent manner.[31] Human neutrophils release elastase to kill tumor cells by liberating the CD95 death domain, which interacts with histone H1 isoforms to selectively eradicate cancer cells.[19] More

[1]Department of Neonatology and Institute of Pediatrics, Children's Medical Center, First Hospital of Jilin University, Jilin University, Changchun, Jilin 130021, People's Republic of China
[2]Department of Molecular Biology, College of Basic Medical Sciences, Jilin University, Changchun, Jilin 130021, People's Republic of China
[3]Department of Immunology, College of Basic Medical Sciences, Jilin University, Changchun, Jilin 130021, People's Republic of China
[4]Department of Pediatric Endocrinology, Children's Medical Center, First Hospital of Jilin University, Jilin University, Changchun, Jilin 130021, People's Republic of China
[5]Lead contact
*Correspondence: wangliy@jlu.edu.cn (L.W.), yancy@jlu.edu.cn (C.Y.)
https://doi.org/10.1016/j.isci.2024.109661

interestingly, it has recently been reported that neutrophils play a killing role for antibody-opsonized cancer cells by trogocytosis (a type of gnawing action).[32] This is a novel way for neutrophils to attack tumor cells in the tumor, which has not been reported before and is worthy of attention.

Trogocytosis is a process previously identified in NK cells and T cells for gnawing target cells.[33–36] Originally, trogocytosis is identified as a phenomenon whereby human NK cells actively capture target cell (K562 cell) membrane fragments.[33] Later on, trogocytosis is documented in T cells, B cells, macrophages, and even cancer cells both *in vitro* and *in vivo*.[35–37] Neutrophils, as the first line of defense in immune cells with phagocytic property, have only recently been mentioned for their trogocytosis on antibody-opsonized tumor cells. At present, it is unclear whether neutrophils use trogocytosis as one of their basic functions to attack tumor cells, especially in the early stage of tumor development. However, the presence of a large number of neutrophils in tumor microenvironment has been largely accepted. Several clues have been found about how neutrophils reach tumor tissues, including chemokines such as CXC motif chemokine ligand 2 (CXCL2) produced by tumor cells or tumor-associated immune cells.[38–40] It is just that the focus has always been on traditional anti-tumor immune cells such as CD8$^+$ T cells and NK cells, as well as antigen-presenting cells (APCs) such as dendritic cells (DCs), for a long time in the field of tumor research, in which neutrophils have been neglected. Promoting the recruitment and activation of CD8$^+$ T cells, NK cells and APCs in the tumor microenvironment are considered to be the key to anti-tumor. We also adopted this idea in our oncological studies and found that the intraperitoneal injection of TLR9 agonist CpG oligodeoxynucleotide (ODN) combined with transforming growth factor β2 (TGF-β2) inhibitor TIO3 in subcutaneous tumor-bearing mice could obviously increase the recruitment and activation of CD8$^+$ T cells and NK cells in the tumor microenvironment while inhibiting tumor growth. The effect of this immunotherapy is depended on the activation of TLR9 because CCT repeat sequence (CCT) ODN, as a TLR9 inhibitory ODN, had no such effect.[41] However, with the deepening of the research, we found that, in the early stage of transplant tumor occurrence, the first immune cells to reach the tumor site were neutrophils, and the application of CpG ODN could also significantly increase the proportion and activation of neutrophils in tumor nodules, and the earlier the application, the stronger the inhibitory effect on tumor growth.[9] This finding aroused our great interest, so we began to pay attention to the relationship between neutrophils and tumor development. Actually, neutrophils are highly heterogeneous and their function can change depending on the environment they live.[12,42] We previously found that the use of TLR9 agonist CpG ODN could significantly reduce the expression level of surface TLR9 (sTLR9) on neutrophils recruited in early tumor nodules, along with slowing tumor growth,[9] but we did not look at whether the trogocytosis of neutrophils also played a role in anti-tumor effect. Now that the trogocytosis of neutrophils on antibody-opsonized tumor cells have been reported, we are very interested to know whether such trogocytosis exists in the early stage of tumors and its relationship with anti-tumor.

Previous studies on the gnawing action of immune cells other than neutrophils have shown that trogocytosis is a behavior that kills target cells, including tumor cells. It has shown that trogocytosed CD8$^+$ T cells, which acquire tumor peptide-major histocompatibility complex from DCs by trogocytosis, can be the killing target of fratricide T cells.[35] Macrophages can kill HER2-overexpressed breast cancer cells by persistently trogocytic attacking.[36] Thus, we may assume that trogocytosis is one of the common ways in which one cell attacks another. Neutrophils, as innate immune cells with phagocytic properties, have been shown to be able to attack antibody-opsonized tumor cells by trogocytosis[32]; it is conceivable that they should also be able to use the trogocytic function to prevent tumor cell expansion when they encounter a transforming tumor cell. It is unclear whether this trogocytic behavior of neutrophils is initially present in early tumors but gradually disappears under the domestication of tumor cells or may have been recalled again under treatment with immunomodulators. The absence of such studies may be related to the lack of suitable models for exploring tumor development in the tumor-initiation stage. Naturally occurring tumors are a chronic disease, and their occurrence is very stealthy. The tumor nodules shown by imaging examination are already tumor tissue formed over a long period of time and are not the initial stage for tumor cells to settle in. Whether neutrophils arrive and play a role in the initial tumor development is unknown. In previous work, our research group found that subcutaneously (s.c.) inoculated tumor cells in mice could induce the formation of early tumor nodules containing a large number of neutrophils as early as 24 h after the inoculation.[9] Although this transplanted tumor model does not explain natural tumorigenesis in mice and humans, it provides a useful model system to elucidate the role and behavior of neutrophils in the innate immune response to tumors, such as trogocytosis.

In this study, we used a mouse subcutaneous transplanted melanoma model and found the presence of trogocytic neutrophils in the early tumor nodule induced by inoculated tumor cells. We also demonstrated that the trogocytosis is a behavior of neutrophils attacking tumor cells. Upregulating the proportion and number of trogocytic neutrophils is conducive to the recruitment and activation of CD8$^+$ T cells and NK cells in the early tumor nodules, and also conducive to inhibiting tumor growth. These results indicate that the presence of trogocytic neutrophils in tumor microenvironment may also contribute to the efficacy of anti-tumor immunotherapy, as in the combination of TLR9 agonist CpG ODN and TGF-β2 inhibitor TIO3. Our results suggest that neutrophils play an important role in shaping the anti-tumor microenvironment at the tumor-initiation stage by trogocytosis, which may have a certain reference value for human anti-tumor immunotherapy.

RESULTS

Early tumor nodules induced by subcutaneous inoculation of B16 melanoma cells in mice and their cell composition

According to the published work of our research group, subcutaneous inoculation of a variety of tumor cells, including B16 melanoma cells (B16 cells), CT26 colon cancer cells (CT26 cells), and H22 liver cancer cells (H22 cells), to mice all induced the formation of tumor nodules containing a large number of neutrophils within 24 h.[9] In this study, we investigated the dynamic changes in the early formation of tumor nodules and their internal cell composition at 1, 6, 12, 24, and 36 h after subcutaneous inoculation at the inner thigh of C57BL/6 mice with GFP-B16 cells (B16 melanoma cells transfected with GFP-encoded gene) (Figure 1A), and the relationship between neutrophils and tumor cells. The medium injection was used as a negative control. When GFP-B16 cells were inoculated for 1, 6, and 12 h, only nodule-like structures with

Figure 1. Tumor nodules induced by subcutaneous inoculation of B16 melanoma cells and their cell composition

(A) GFP-B16 cells. B16 melanoma cells were stably transfected with GFP-coding gene and termed as GFP-B16 cells.

(B) The morphology, size, and GFP$^+$ nodule cell counts of subcutaneous nodules 1–36 h after inoculation with GFP-B16 cells. Medium injection was as control. The GFP$^+$ nodule cells were counted by flow cytometry. Yellow arrow, nodule-like or nodule; Yellow circle, medium injection site.

(C) The cell composition of tumor nodules at 24 h after inoculation.

(D) Immunofluorescence results of homogenate cells of tumor nodules at 24 h after inoculation. The tumor nodule cells were stained with Evans blue and then observed under the fluorescence microscope. The green represents GFP-B16 cells. The red represents the cells stained by Evans blue.

(E) Immunofluorescence results of frozen sections of tumor nodules at 24 h after inoculation. The green color represents GFP-B16 cells. The yellow color represents the cells stained by PE-labeled anti-Ly6G antibody.

(F) The percentages of Ly6G$^+$ neutrophils, GFP$^+$ tumor cells, and F4/80$^+$ macrophages in tumor nodules at different times after inoculation.

(G) The expression of CXCL2 in the cultured B16 cells and the nodule cells 1 h and 6 h after inoculation. The cultured B16 cells were indirectly stained with Rabbit Anti-Mouse CXCL2 mAb and FITC-Goat Anti-Rabbit IgG intracellularly. The nodule cells were surface stained and then intracellularly stained. Flow cytometry was used for the detection. Dynamic data are from one experiment, and other data are from one of three experiments. *In vivo* experiment of Figures 1B–1D, 1F, and 1G right, each dot in the histogram represents one mouse; and *in vitro* experiment of Figure 1G left, each dot in the histogram represents the cultured cells in one well. Data are expressed as mean ± SD, *$p < 0.05$, **$p < 0.01$, ***$p < 0.001$, ****$p < 0.0001$.

a size of 1–5 mm^2 were seen by the naked eye, and no typical nodules were formed. 24 h after the inoculation, a typical grayish-white soft nodule with capillary embedding was formed, approximately 17 mm^2 in size. No nodule-like structure or nodules were observed at each time point of the injection medium site (Figure 1B, left). These results indicated that nodules were induced by inoculated tumor cells but not injection itself, therefore termed as early tumor nodules. The number of GFP$^+$ cells in nodule-like tissues or nodules detected by flow cytometry gradually increased within 1–12 h and then rapidly decreased, from 150,000 at 12 h to about 50,000 at 24–36 h (Figure 2B, right), indicating that GFP$^+$ tumor cells in nodules may be reduced by death.

We then analyzed the cell composition in tumor nodules at 24 h post-inoculation using flow cytometry. We found that Ly6G$^+$ neutrophils were the main immune cell type in tumor nodules, accounting for 65% of the total cell population, followed by 12% F4/80$^+$ macrophages, 5% NK1.1$^+$ NK cells, 1% CD19$^+$ B cells, and 1% CD3$^+$ T cells. All leukocytes accounted for about 84% of the tumor nodule cells, while GFP$^+$ tumor cells accounted for 15% and other unknown cells accounted for only 1%. In contrast, CD45$^+$ leukocytes accounted for only 12.52% of the tissue-derived cells at the site of medium injection, among which CD3$^+$ T cells were the main cells, accounting for about 5%, and other unknown cells except CD45$^+$ leukocytes accounted for 87.48% of the total tissue cells (Figure 1C). By using immunofluorescence assays, we found that GFP$^+$ cells were present in the nodules, accounting for approximately 15% (Figure 1D), and clearly seen on frozen sections (Figure 1E). These results suggest that neutrophils are the primary immune cell type in the early tumor nodule. We further analyzed the proportions of Ly6G$^+$ neutrophils, F4/80$^+$ macrophages, and GFP$^+$ cells in the nodules at different time points after inoculation. We found that the proportions of neutrophils and macrophages in cells of the nodule-like tissue or nodules were near or less than 10% at 1 h post-inoculation, but the proportion of neutrophils increased to 65% while the proportion of macrophages remained below or at 10% at 6–36 h post-inoculation. The proportion of GFP$^+$ cells in those cells was highest at 1 h, about 50%, and gradually decreased, remaining at about 15% at 24–36 h post-inoculation (Figure 1F, left). To exclude the possible influence of dead cells on flow cytometry results, we labeled the cells with dead cell marker dye 7-amino-actinomycin (7AAD) and then performed the flow cytometry. From the proportion and number of three group cells in the nodules, although there were some differences, especially the number of Ly6G$^+$ cells and GFP$^+$ tumor cells decreased over time, the overall trend was similar to the earlier results, indicating that the dead cells had no significant impact on the flow cytometry results in this study (Figure 1F, right). These results indicate that subcutaneous inoculation of B16 melanoma cells leads to the formation of early tumor nodules and neutrophils are dominant immune cells in the nodules. The recruitment of a large number of neutrophils to the site of tumor cell inoculation may be related to the local production of chemokines such as CXCL2.[38–40] To prove this deduction, we first detected CXCL2 production in cultured B16 cells by flow cytometry and found that B16 cells expressed CXCL2 (Figure 1G, left). Then, we tested the CXCL2 expression in nodule-like tissue cells at 1 h and 6 h after inoculation of B16 cells or injection of medium by flow cytometry. The results showed that, when B16 cells were inoculated for 1 h, the cells expressing CXCL2 in nodule-like tissue were mainly CD45$^-$ cells. If it was compared with that of the medium (Med) group, CXCL2 could basically be determined to be mainly produced by tumor cells. However, when B16 cells were inoculated for 6 h, CXCL2-producing cells in nodule-like tissue became mainly CD45$^+$ cells, and Ly6G$^+$ cells were dominant (Figure 1G, right). It is suggested that chemokines produced by the inoculated tumor cells may be the first driving force. Chemokine produced by leukocytes (especially recruited neutrophils) in nodules may provide positive feedback driving force.

Neutrophils in early tumor nodules possessed the ability to engulf tumor cells

To determine whether neutrophils in early tumor nodules could attack tumor cells, considering that, in addition to neutrophils, macrophages had about 10% in the nodule and tumor cells were GFP positive (GFP$^+$), and these two groups of cells could be represented by GFP$^+$ if they engulfed tumor cells, we firstly detected the proportion of GFP$^+$ neutrophils (GFP$^+$Ly6G$^+$) and GFP$^+$ macrophages (GFP$^+$F4/80$^+$) in nodule-like tissue or tumor nodules at 1–36 h after GFP-B16 cell inoculation by flow cytometry. The results showed that, in nodule cells, the percentage of GFP$^+$Ly6G$^+$ cells was 2.5% at 1 h after inoculation, increased to 13% at 6 h, and then decreased from 8% to 4% during 12–36 h, being about 5% at 24 h. In contrast, the percentage of GFP$^+$F4/80$^+$ cells of the nodule cells remained at or below 1%–2% at all time points (Figure 2A, left). In addition to neutrophils and macrophages, T cells, B cells, and NK cells have also been reported to have trogocytosis. Therefore, we used flow cytometry to detect different GFP$^+$ immune cells in nodules. The results showed that the proportion and number of GFP$^+$NK1.1$^+$
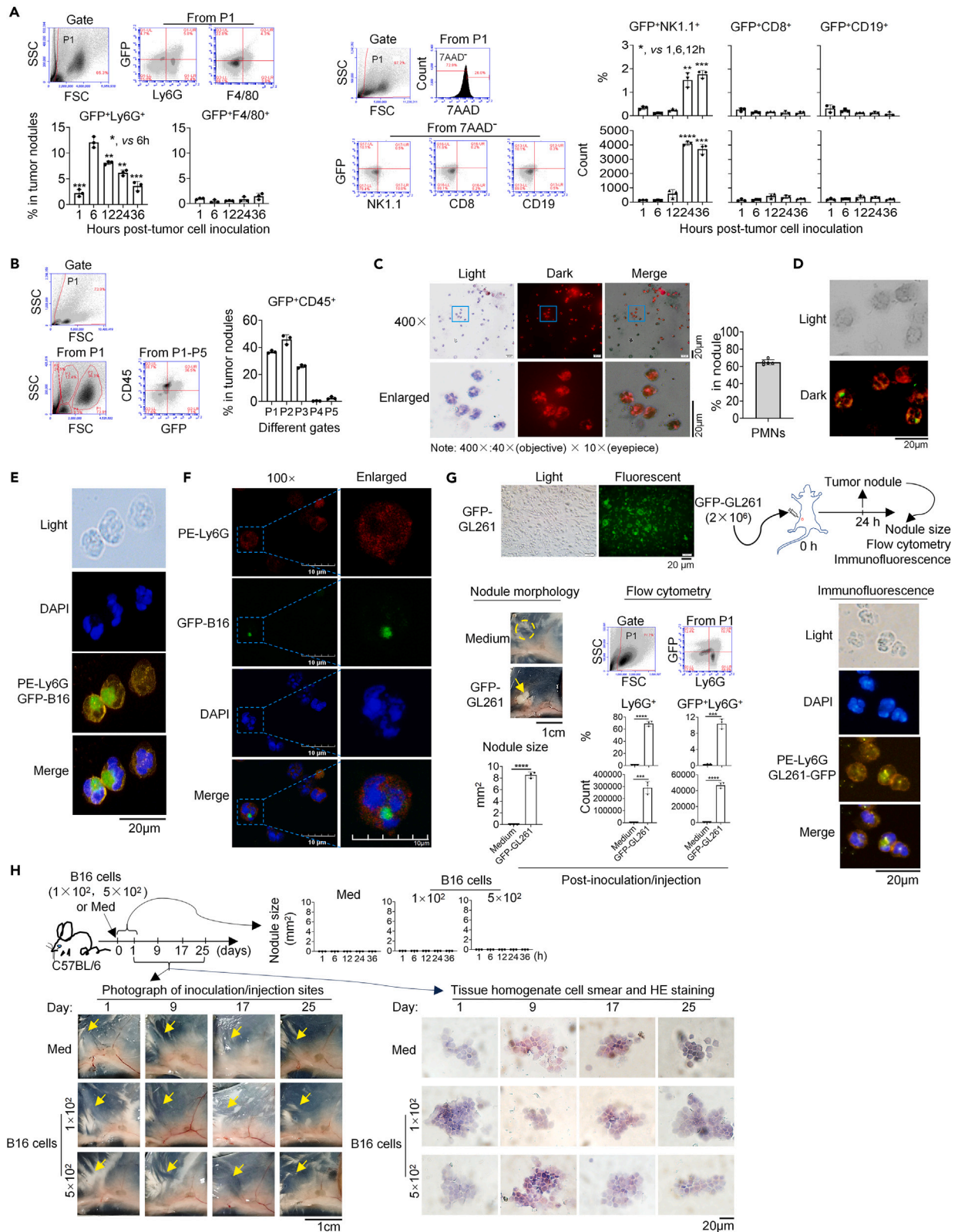
Figure 2. Detection of GFP⁺ neutrophils/macrophages in tumor nodules

(A) GFP⁺ immune cells, including Ly6G⁺, F4/80⁺, NK1.1⁺, CD8⁺, and CD19⁺ cells in tumor nodules, were detected by flow cytometry at different times after tumor cell inoculation.

(B) The percentage of GFP⁺CD45⁺ cells in different gated tumor nodule cells 24 h after the inoculation.

(C and D) (C) PMNs in tumor nodule cells and (D) PMNs with green fluorescence. The tumor nodule cells stained by Evans blue and H&E staining were detected under the microscope (light) or fluorescence microscope (dark), respectively. Red, the cells stained by Evans blue. Green, GFP-B16 cells. Purple, cells stained by H&E.

(E) Ly6G⁺ cells with green fluorescence in tumor nodule cells observed under fluorescence microscope.

(F) Ly6G⁺ cells with green fluorescence in tumor nodule cells observed under confocal fluorescence microscope.

(G) The presence of trogocytic neutrophils in early tumor nodules induced by a subcutaneous inoculation of murine glioma cell line GL261 cells transfected with GFP-encoded gene (GFP-GL261 cells). Medium injection was as control. Yellow arrow, nodule-like or nodule; Yellow circle, medium injection site.

(H) Observation of the tumor formation by subcutaneously inoculating a few hundred B16 melanoma cells in mice. Dynamic data are from one experiment, and other data are from one of three experiments. *In vivo* experiment of Figures 2A–2C, 2G, and 2H, each dot in histogram represents one mouse. Data are expressed as mean ± SD, *$p < 0.05$, **$p < 0.01$, ***$p < 0.001$, ****$p < 0.0001$.

cells in nodules increased from less than 0.5% and 1000 to nearly 2% and 4000, respectively, at the time of typical nodule formation at 24 h and 36 h after inoculation of GFP-B16 cells. In contrast, the proportion and number of GFP⁺CD8⁺ and GFP⁺CD19⁺ cells were almost undetectable in nodules at all time points (Figure 2A, right). Although the proportion of GFP⁺Ly6G⁺ cells at the 6 h tumor cell inoculation site was the highest, no typical nodules were formed at this time, and the local tissue was liquefied, making it difficult to conduct standardized experimental operations. Typical membrane-coated nodules did not form until 24 h after tumor cell inoculation. Therefore, in order to facilitate the operation and reduce the error between experiments, we selected tumor nodules inoculated with tumor cells for 24 h as the study object in the follow-up experiment. Next, based on the fact that CD45 is a surface marker of all leukocytes, different leukocyte populations can be analyzed by gating strategies in flow cytometry according to cell size and complexity. In addition, GFP is a marker of GFP-B16 cells, and, if GFP appears in leukocytes, it can be labeled as GFP⁺CD45⁺ cells and indicates these leukocytes have engulfed tumor cells. Based on this characteristic of flow cytometry, we used side scatter (SSC) and forward scatter (FSC) to gate live cells (P1) in tumor nodule cells and then gate different morphologic populations of neutrophil-rich cells (P2, P3, and P5), and lymphocyte-rich cell population (P4) from P1. Through the analysis of GFP⁺CD45⁺ cells in P1-P5 gated cells, we found that GFP⁺CD45⁺ cells were mainly distributed in P2 and P3 gated cell populations of tumor nodule cells at 24 h of GFP-B16 cell inoculation, indicating that neutrophils in tumor nodules engulfed tumor cells (Figure 2B). The fluorescence microscope observation confirmed the presence of PMNs in tumor nodules 24 h post-inoculation, accounting for about 65% of total cells (Figure 2C). The green fluorescence was also visible in the PMNs (Figure 2D), indicating that neutrophils might have engulfed tumor cells. To clarify the relationship between neutrophils and tumor cells in tumor nodules, we conducted a detection with a fluorescence microscopy and found that GFP⁺ tumor cells existed in Ly6G⁺ neutrophils (Figure 2E), suggesting that neutrophils engulfed tumor cells. To reduce the possible interference of multiple staining on the earlier observation and confirm the localization of tumor cells in neutrophils, we did another detection with a confocal fluorescence microscopy and found that GFP⁺ tumor cells were indeed present in neutrophils and were located in the cytoplasm of neutrophils (Figure 2F). These findings suggest that neutrophils are main immune cells in tumor nodules to have the ability to engulf tumor cells at the early stage of tumor formation.

We also inoculated mice s.c. with GL261 glioma cells transfected with GFP-encoded gene (GFP-GL261 cells) and found that nodules also formed 24 h after inoculation containing about 65% neutrophils and 10% GFP⁺Ly6G⁺ cells, the latter of which were also visible under fluorescence microscopy (Figure 2G). These results suggest that the presence of trogocytic neutrophils in early tumor nodules possesses a generality. Considering that the natural tumor formation is a long-term process, we inoculated 1×10^2 and 5×10^2 GFP-B16 cells s.c. in C57BL/6 mice to observe whether there were differences in trogocytic neutrophils during the long-term tumor growth. Tumor nodules were examined at the early stage of tumor formation. The tumor size and neutrophil recruitment were measured at subsequent times. The results showed that when 100 and 500 tumor cells were given s.c. into mice, no nodules were found at the inoculation site 6–36 h after inoculation. After that, we also found no palpable tumor. To confirm the absence of tumors, we examined the subcutaneous tissue of inoculation site at day 1, 9, 17, and 25 post-inoculations, and no tumor was found. We also did not find any neutrophil at the tissue of inoculation site by staining of biopsy tissue slice (Figure 2H). This suggests that it is difficult to simulate the chronic long-term growth process of tumors with a small number of transplanted tumor cells.

Neutrophils in early tumor nodules attacked tumor cells in a variety of ways leading to their death

To better understand the attack mode of neutrophils on tumor cells in tumor nodules, we conducted a thorough analysis of cell morphology using H&E and Evans blue staining. Our observations revealed the presence of scattered or clustered tumor nodular cells with nuclei compressed to the edges. Under fluorescence microscope, we found GFP⁺ cells present between or even inside the red color cells stained with Evans blue (Figure 3A, up). We observed that some GFP⁺ cells were adhering to other cells, while others fused with other cells (Figure 3A, down), suggesting that there may be cells in tumor nodules that can eat tumor cells. Given the abundance of neutrophils in tumor nodules, we used phycoerythrin (PE)-labeled anti-Ly6G antibody to stain the nodule cells and observed under the fluorescence microscope to identify any Ly6G⁺ neutrophils (yellow color) that could eat GFP⁺ tumor cells (green color). Our observations confirmed that neutrophils in tumor nodules were indeed eating or had eaten tumor cells. Based on our microscopic observations, we described these phenomena as neutrophils and tumor cells living independently (scatter), adhering to each other (attach), neutrophils gnawing on the tumor cells (nibble), or neutrophils
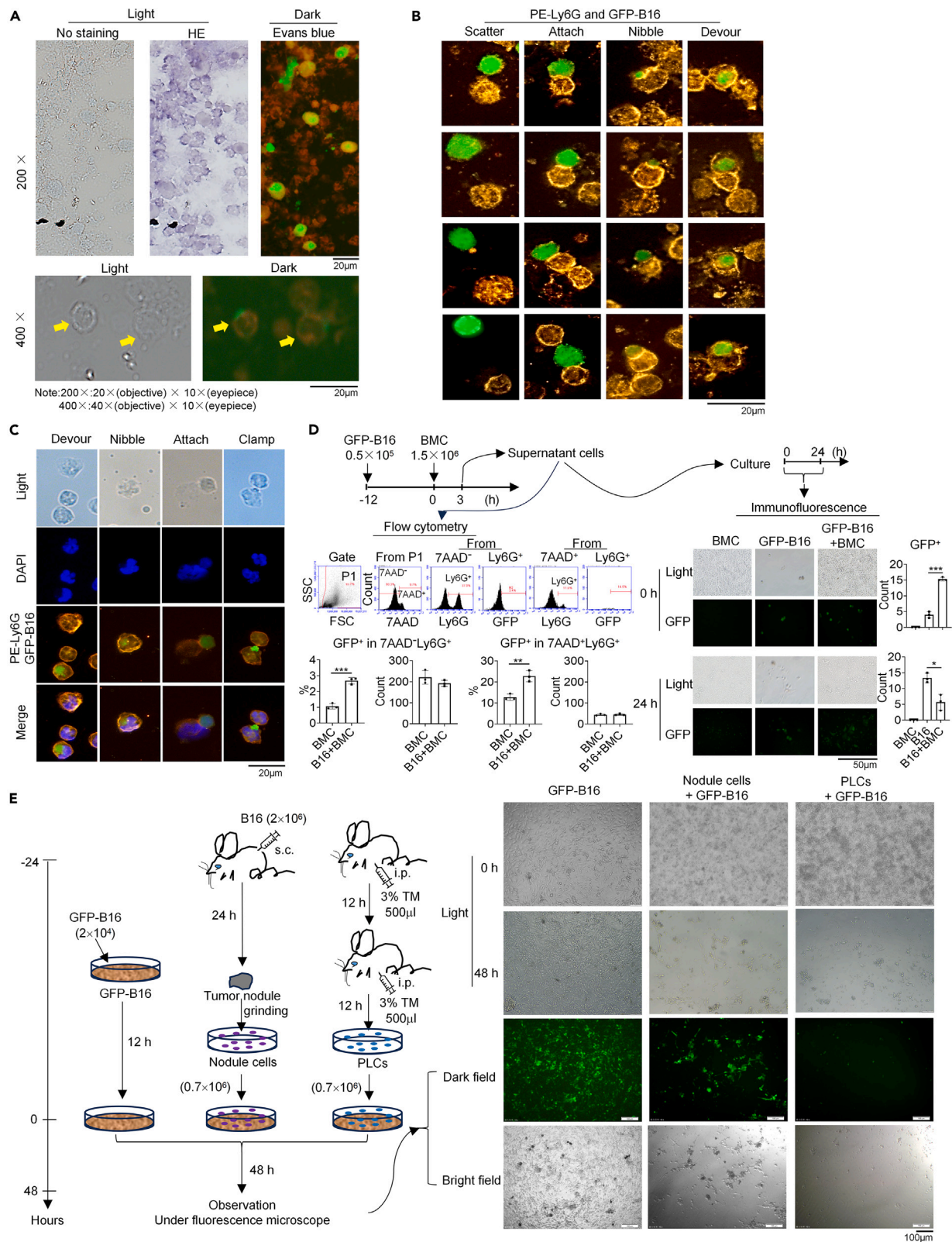
Figure 3. Neutrophils in tumor nodules that attack tumor cells

(A) Smear of cells from tumor nodules 24 h post GFP-B16 cell inoculation. The tumor nodule cells were stained by Evans blue and H&E staining, and then observed under the fluorescence microscope. Red, the cells stained by Evans blue. Green, GFP-B16 cells. Purple, cells stained by H & E.

(B) Relationship between neutrophils and tumor cells in tumor nodules at 24 h after GFP-B16 cell inoculation. The tumor nodule cells were stained with PE-labeled anti-Ly6G antibody followed by observation under the fluorescence microscope.

(C) Neutrophils and tumor cells in tumor nodules at 24 h after GFP-B16 cell inoculation. The tumor nodule cells were stained with PE-labeled anti-Ly6G antibody and DAPI followed by observation under the fluorescence microscope.

(D) The *in vitro* experiment system using GFP-B16 cells co-cultured with bone marrow cells (BMCs) to track the fate of tumor cells after trogocytosis by observing the survival and growth of suspended tumor cells derived from the co-culture system after re-cultured. In co-culture system, the proportion and number of trogocytic neutrophils between BMC group and B16+BMC group were compared. In following re-culture system, the numbers of alive GFP$^+$ cells between BMC group, B16 group and B16+BMC group were tracked. Each dot in histogram represents the cultured cells in one well.

(E) The *in vitro* tumor cell killing assay. Neutrophil (about 65%)-rich nodule cells from 24 h tumor nodules in the killing assay were as effector cells and co-cultured with GFP-B16 cells for 48 h to observe the survival of GFP-B16 cells. Thioglycollate medium (TM) induced mouse peritoneal lavage cells (PLCs) were as control of effector cells. Data are from one of two experiments. Data are expressed as mean $\pm$ SD, *$p < 0.05$,**$p < 0.01$, ***$p < 0.001$.

engulfing the tumor cells (devour) (Figure 3B). When the nuclei of tumor nodule cells were stained with DAPI, we clearly observed that the gnawing (nibble), engulfing (devour), attaching, and even clamping to tumor cells were the work of neutrophils (Figure 3C). These results suggest that neutrophils in tumor nodules can attack tumor cells in a variety of ways, including devouring, nibbling, and even clamping, simply named as trogocytosis.

To track the fate of tumor cells after trogocytosis of neutrophils, we conducted an *in vitro* experiment system using GFP-B16 cells co-cultured with bone marrow cells (BMCs) to observe the survival and growth of suspended tumor cells derived from the co-culture system after re-culture. The results showed that GFP$^+$Ly6G$^+$ cells were present in the suspended cells floating in the culture medium after 3 h co-culture of GFP-B16 cells with BMCs, suggesting that tumor cells were gnawed possibly by neutrophils in BMCs. After these suspended cells were cultured for another 24 h, the number of GFP-B16 cells in suspended cells of the co-culture system was obviously reduced (Figure 3D), indicating that the survival and growth ability of these tumor cells was weakened. Then, to prove that trogocytosis could kill tumor cells, we harvested the neutrophil (about 65%)-rich nodule cells from 24 h tumor nodules of B16 cell-inoculated mice as effector cells and co-cultured with GFP-B16 cells for 48 h to observe the survival of GFP-B16 cells. GFP-B16 cells were cultured alone or co-cultured with thioglycollate medium (TM)-induced mouse peritoneal lavage cells (PLCs) as controls. The results showed that the number of GFP-B16 cells co-cultured with nodule cells was significantly reduced compared with that cultured alone, while the number of GFP-B16 cells co-cultured with PLCs completely disappeared (Figure 3E). This result seems to indicate that trogocytosis, as a way of neutrophil activation, can kill tumor cells, because of the presence of trogocytic neutrophils in 24 h tumor nodules and a large number of activated neutrophils in PLCs.

Effect of immunomodulators with anti-tumor effects on the proportion of trogocytic neutrophils in early tumor nodules

Based on the aforementioned findings, we speculated that increasing the proportion of trogocytic neutrophils in early tumor nodules might contribute to promoting the establishment of an anti-tumor microenvironment. To investigate this, based on our previous finding that the combination of TLR9 agonist CpG ODN and TGF-β2 antisense deoxyoligonucleotide TIO3 (CpG+TIO3) by intraperitoneal injection could exert a significant anti-tumor growth,[41] we used CpG+TIO3 to treat the model mice through intraperitoneal injection at the same time of the subcutaneous inoculation of GFP-B16 melanoma cells. The treatment with PBS was used as control. After 24 h of the inoculation, the subcutaneous early tumor nodules were acquired and analyzed (Figure 4A). The results showed that the early tumor nodule was formed s.c. at the site of tumor cell inoculation in both groups, with similar sizes and weights (Figure 4B). The proportion of trogocytic neutrophils in the tumor nodule cells was significantly increased, from 5% to 10% in the CpG+TIO3 group compared to that in PBS group (Figure 4C). We then analyzed the proportion of Ly6G$^+$ cells and GFP$^+$Ly6G$^+$ cells in the nodules by flow cytometry. We found that the proportion of both Ly6G$^+$ cells and GFP$^+$Ly6G$^+$ cells in CpG+TIO3 group increased significantly compared to that in the PBS group, by about 15% and 1.5–2 times, respectively (Figure 4D). Further analysis by marking GFP$^+$Ly6G$^+$ cells (green) and GFP$^-$Ly6G$^+$ cells (black) in living cells (P1) of tumor nodules also revealed a significant increase of GFP$^+$Ly6G$^+$ cells in the CpG+TIO3 group (Figure 4E). These results suggest that CpG+TIO3 can increase the proportion of trogocytic neutrophils in early tumor nodules, which may be one of the reasons for its anti-tumor effect. To verify this, we used CCT ODN (a TLR9 inhibitory ODN) combined with TIO3 (CCT+TIO3, which was shown to have no anti-tumor effect in our previous work[41]) to treat the model mice as earlier and detect tumor nodules and their proportion of Ly6G$^+$ cells and GFP$^+$Ly6G$^+$ cells at 24 h after inoculation. The weights of tumor nodules in the CCT+TIO3 group were similar to those in the PBS group (Figure 4F, left). Meanwhile, the proportions of Ly6G$^+$ cells and GFP$^+$Ly6G$^+$ cells in tumor nodules of the CCT+TIO3 group were also similar to the proportion in the PBS group (Figure 4F, right). This result further supports the earlier conclusion that immunomodulators with anti-tumor effects can increase the proportion of trogocytic neutrophils in early tumor nodules.

Effect of increasing trogocytic neutrophils on the recruitment or activation of other immune cells in early tumor nodules

To test whether increasing trogocytic neutrophils could upregulate the proportion of other anti-tumor immune cells in early tumor nodules, we injected CpG+TIO3, CCT+TIO3, or PBS intraperitoneally (i.p.) into model mice simultaneously inoculated s.c. with B16 cells. We then measured the proportion of CD8$^+$ T cells and NK cells and their interferon (IFN)-γ production in 24 h tumor nodules by flow cytometry. Results showed that the size of tumor nodules in CpG+TIO3, CCT+TIO3, and PBS groups were similar, but there were obviously differences in the
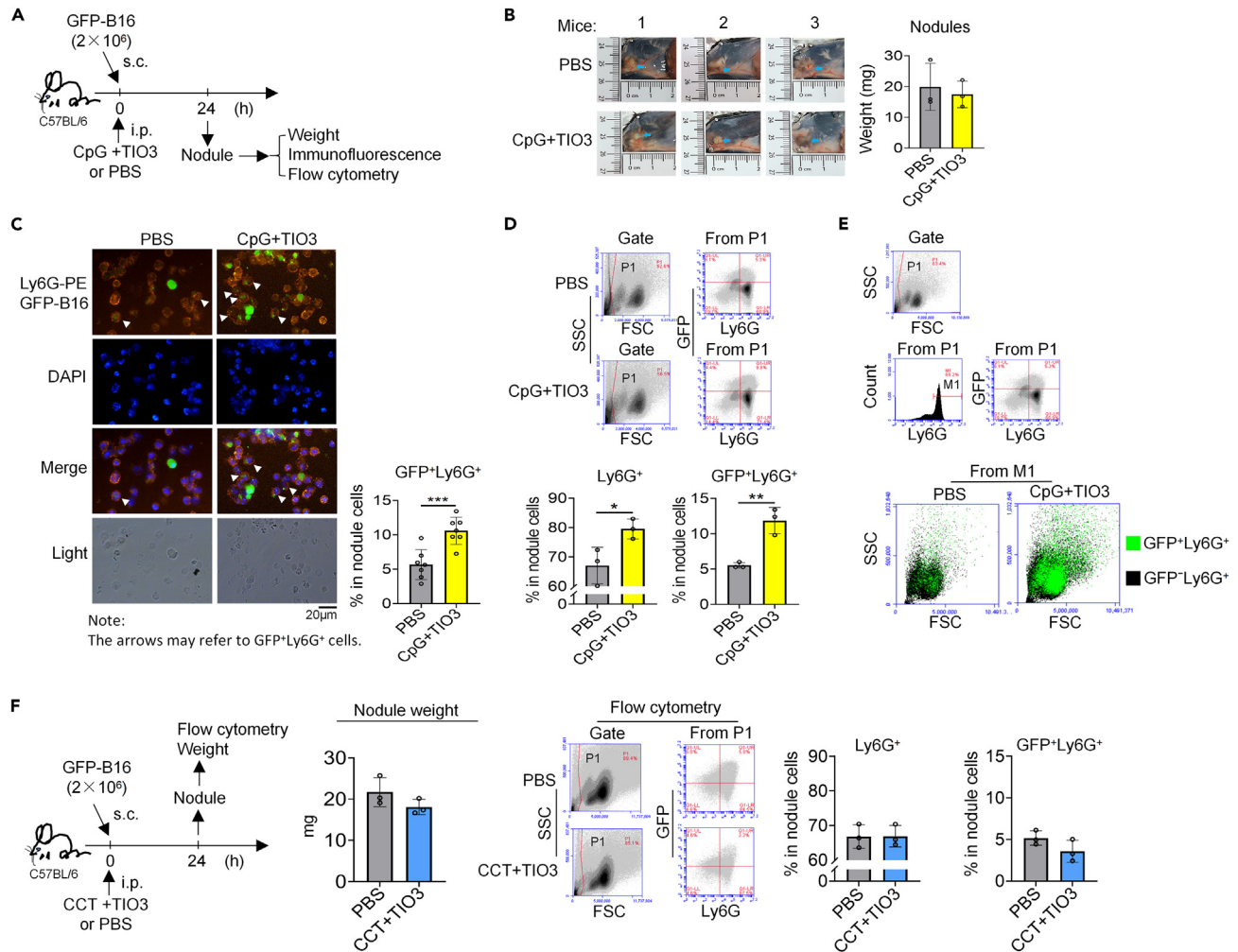
Figure 4. The impact of systemically applied ODNs on the proportion of neutrophils that engulf or gnaw tumor cells in tumor nodules

(A) The experiment procedure for intraperitoneal administration of CpG ODN+TIO3 (CpG+TIO3) to treat mice that were subcutaneously inoculated with GFP-B16 cells.

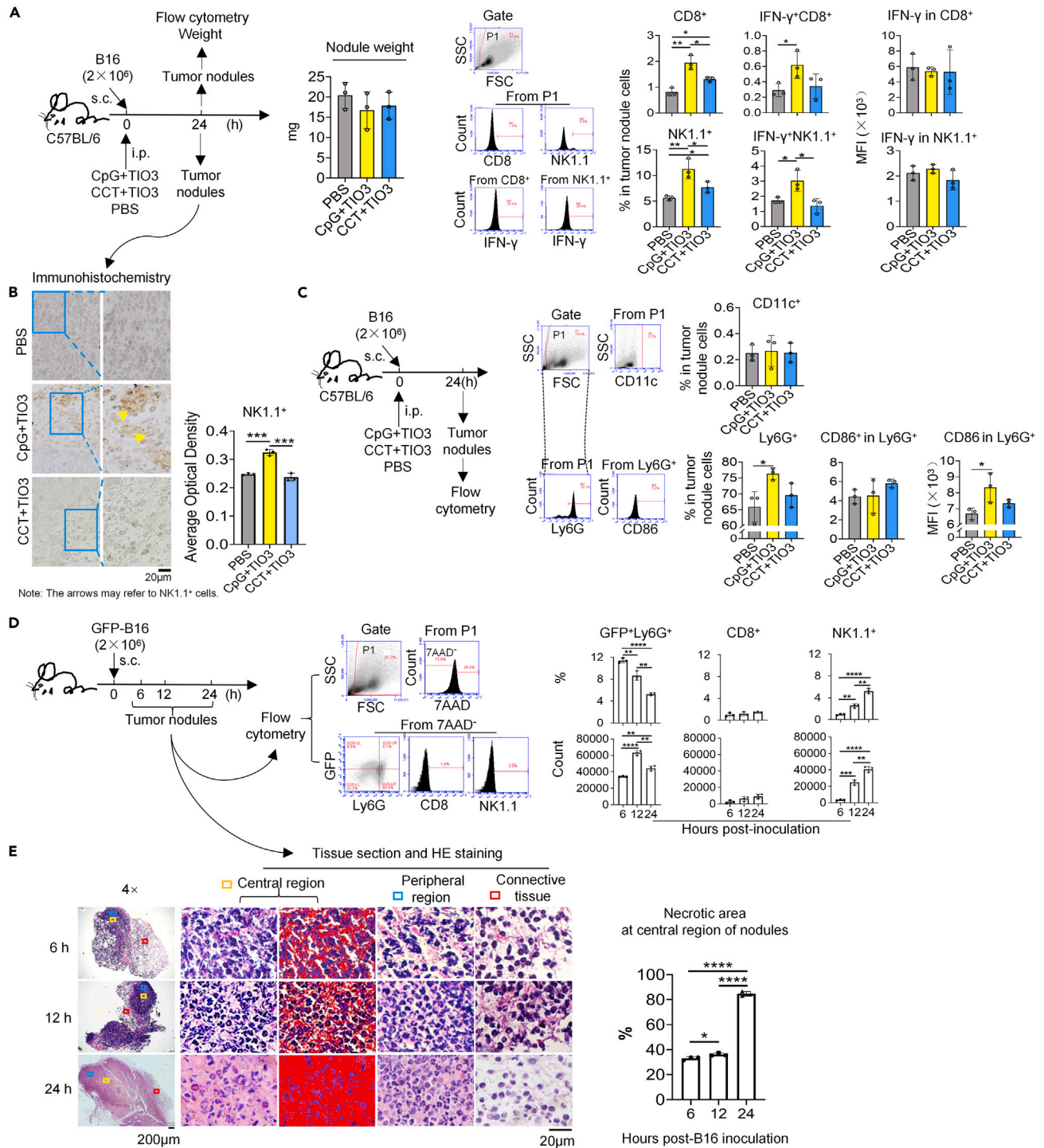(B) The tumor nodules of mice in both the CpG+TIO3 and PBS groups.

(C) The percentages of trogocytic neutrophils in tumor nodules of CpG+TIO3 or PBS groups, as determined through a relative quantitative method based on fluorescent imaging.

(D) The percentages of Ly6G$^+$ cells and GFP$^+$Ly6G$^+$ cells in tumor nodules of mice in both the CpG+TIO3 and PBS groups, as detected by flow cytometry.

(E) The percentages of GFP$^+$Ly6G$^+$ cells in tumor nodules of mice in both the CpG+TIO3 and PBS groups, as detected by flow cytometry.

(F) The percentages of Ly6G$^+$ cells and GFP$^+$Ly6G$^+$ cells in tumor nodules of mice in both the CCT ODN+TIO3 (CCT+TIO3) and PBS groups, also detected by flow cytometry. The left part depicts the experiment procedure and the tumor nodular weight, while the percentages of Ly6G$^+$ cells and GFP$^+$Ly6G$^+$ cells in tumor nodules are shown in the right of the figure. In all the experiments, both experimental and control, there were three mice in each group. Data are from one of two experiments. Data are expressed as mean ± SD, *$p < 0.05$,**$p < 0.01$, ***$p < 0.001$.

proportion and activation of CD8$^+$ T cells and NK cells in the nodules. CpG+TIO3 could significantly increase the proportion of CD8$^+$/NK1.1$^+$ cells and IFN-γ^+CD8$^+$/NK1.1$^+$ cells although it did not upregulate the expression levels of IFN-γ in CD8$^+$ T cells and NK cells. Compared with that in PBS and CCT+TIO3 groups, the proportion of CD8$^+$/NK1.1$^+$ cells and IFN-γ^+CD8$^+$/NK1.1$^+$ cells increased by about 1 time, respectively (Figure 5A). This result was also confirmed by immunohistochemical staining of paraffin sections of tumor nodules, in which CpG+TIO3 increased NK cells in tumor nodules (Figure 5B). By detecting CD11c$^+$ cells, Ly6G$^+$ cells, and CD86 expression on Ly6G$^+$ cells in the 24 h tumor nodules, it was found that CpG+TIO3 significantly increased the proportion of Ly6G$^+$ cells and the expression level of CD86 on Ly6G$^+$ cells, but not the proportion of CD11c$^+$ cells (Figure 5C). These results suggest that increasing neutrophils and trogocytic neutrophils in early tumor nodules is conducive to the arrival and activation of CD8$^+$ T cells and NK cells, and those neutrophils also seem to play an antigen-presenting role.

Figure 5. Effect of increasing neutrophils and trogocytic neutrophils on the recruitment or activation of other immune cells in early tumor nodules

(A) The impact of systemically applied ODNs on the proportion of CD8^{+} T cells, NK cells, and their activation in early tumor nodules at 24 h after B16 cell inoculation. The ODNs or PBS were injected intraperitoneally (i.p.) to mice at same time of s.c. inoculation of B16 cells. The CD8^{+} T cells and NK cells were detected by flow cytometry.

(B) Detection of NK cells in paraffin sections of the 24 h tumor nodules by immunohistochemistry staining.

(C) Detection of CD11c^{+} and Ly6G^{+} cells and the CD86 levels on Ly6G^{+} cells in the 24 h tumor nodules.

Figure 5. *Continued*

(D) Time kinetics of the proportion and number of CD8$^+$ T cells, NK cells, and GFP$^+$Ly6G$^+$ cells in tumor nodules.

(E) Time kinetics of pathological changes of nodule-like or nodule tissues. The H&E-stained tissue sections were detected under the microscope. In all the experiments, both experimental and control, there were three mice in each group. Dynamic data are from one experiment, and other data are from one of two experiments. Data are expressed as mean ± SD, *$p < 0.05$,**$p < 0.01$, ***$p < 0.001$, ****$p < 0.0001$.

To confirm that the changes of trogocytic neutrophils affected the CD8$^+$ T cells and NK cells in early tumor nodules, we detected the time kinetics of the proportion and number of CD8$^+$ T cells, NK cells, and GFP$^+$Ly6G$^+$ cells in tumor nodules. The results showed that the proportion of GFP$^+$Ly6G$^+$ cells in the nodules was the highest at 6 h and 12 h, about 8%–12%, and at 24 h it was about 6%, which was about 1 time lower than that at 12 h. The proportion of NK1.1$^+$ cells gradually increased over time and was the highest at 24 h (about 6%), which was 2 times higher than that at 12 h. The number of GFP$^+$Ly6G$^+$ cells was similar at 6 h and 24 h, and the highest at 12 h was about 1 time higher than that at 6 h and 24 h. The number of NK1.1$^+$ cells gradually increased over time, reaching a maximum value at 24 h, about 2 times than that at 12 h. Throughout the process, the proportion and number of CD8$^+$ T cells were at very low levels (Figure 5D). The increase of GFP$^+$Ly6G$^+$ cells in nodules was earlier than that of NK1.1$^+$ cells, suggesting that trogocytic neutrophils may play a role in inducing NK cells to enter the nodule. To prove that the decrease in the proportion and number of trogocytic neutrophils in 24 h tumor nodules compared with those in short-term nodules might be due to the fact that neutrophils themselves died while killing tumor cells or imply that neutrophils could kill tumor cells in a suicidal way, we dynamically detected the pathological changes of nodules through H&E staining of tissue sections. We analyzed the central, peripheral, and outermost connective tissue regions of the nodules. The results showed that the three regions seen at 6 h, 12 h, and 24 h were basically neutrophils and large tumor cells. The difference was that the cell density in the central region gradually decreased over time. The necrotic area in the central region of the nodules at 24 h was significantly larger than that at the other two time points, while no significant necrotic phenomenon was found in the peripheral region and the connective tissue region (Figure 5E). This result is consistent with the reduction of GFP$^+$Ly6G$^+$ cells in 24 h nodule, suggesting that necrosis might be related to the trogocysis of neutrophils.

Effects of immunomodulators with upregulating the proportion of trogocytic neutrophils on tumor growth in mice

In the earlier studies, we have been focusing on changes in early tumor nodules of mice inoculated s.c. with tumor cells. Here, we wanted to see if affecting early tumor nodules could affect subsequent tumor growth in tumor-bearing mice. Considering that natural tumor growth is a slow process, we first explored the minimum number of inoculating B16 cells that could form palpable tumors around 10 days in mice after inoculation. It was found that mice inoculated with 5×10^5 B16 cells developed tumors by day 9 after inoculation, while mice inoculated with 2×10^6 B16 cells or 1×10^5 B16 cells developed tumors either too early (day 2 after inoculation) or too late (over 14 days post-inoculation). When 2×10^6 B16 cells were inoculated in mice, the tumors appeared on day 2 after inoculation and had grown to nearly 2,000 mm^3 by 14 days (Figure 6A). Therefore, in the follow-up *in vivo* experiment, we selected 5×10^5 B16 cells to inoculate mice s.c.

To test immunomodulators with upregulating the proportion of trogocytic neutrophils on tumor inhibition, we began the administration of CpG+TIO3, CCT+TIO3, or PBS i.p. at the same time of subcutaneous inoculation of B16 melanoma cells, once every other day, four times in total, to observe the tumor growth and survival of mice (Figure 6B). The results showed that CpG+TIO3 could significantly inhibit tumor growth in mice; that is, the tumor appeared late, grew slowly, and was small in size, which was statistically significant compared with the tumor growth in mice of the PBS and CCT+TIO3 groups ($p = 0.0012$ and $p = 0.027$). On day 17 after tumor cell inoculation, the mean tumor volume in mice of the CpG+TIO3 group was less than 1,000 mm^3, which was only 1/6 of that in the PBS group and 1/3 of that in the CCT+TIO3 group. There was no significant difference in tumor growth in mice between the PBS and CCT+TIO3 groups. In addition, the survival time of mice in the CpG+TIO3 group was also significantly longer than that in the PBS and CCT+TIO3 groups ($p = 0.0043$ and $p = 0.0135$). On the day 28 after tumor cell inoculation, the survival rate of mice in the CpG+TIO3 group was 83.3%, while only 27.7% of mice in the CCT+TIO3 group survived, and all mice in the PBS group died (Figure 6B). These results suggest that immunomodulators capable of increasing the proportion of trogocytic neutrophils in early tumor nodules can also induce the inhibition of tumor growth, which may be related to its induction on the formation of an anti-tumor immune microenvironment.

Effect of reducing the recruitment of neutrophils in tumor nodules on nodule size and nodule cell composition

In order to directly demonstrate the relationship between neutrophils and their anti-tumor activity, we used RNA interference (RNAi) to downregulate the expression of CXCL2 (a chemokine for recruiting neutrophils) in tumor nodules and observe whether neutrophils, CD8$^+$ T cells, and NK cells in tumor nodules changed. We first transfected three *Cxcl2* siRNAs (SIR-93, SIR-131, and SIR-207) and one control siRNA (SIR-Ctrl) into B16 cells and detected the *Cxcl2* mRNA levels in the transfected cells by quantitative reverse-transcription PCR (RT-qPCR). The results showed that compared with SIR-Ctrl the expression of *Cxcl2* could be significantly downregulated with these three *Cxcl2* siRNAs after transfection for 7 h (Figure 7A). Next, SIR-93 and SIR-Ctrl were selected for *in vivo* experiments, and siRNA was injected s.c. at the same site while GFP-B16 cells were inoculated. 24 h after inoculation, tumor nodules were examined by RT-qPCR and flow cytometry (Figure 7B). We found that tumor nodules in mice given SIR-93 were significantly enlarged (Figure 7C), but their *Cxcl2* mRNA levels were significantly decreased (Figure 7D). We then examined the cell composition and trogocytic immune cells of the tumor nodules, with particular focus on the recruitment and trogocytosis of neutrophils and CD8$^+$ T cells and NK cells. We found that the number of live cells isolated from tumor nodules in mice treated with *Cxcl2* siRNA was similar to that in the control group, but GFP$^+$ tumor cells were obviously
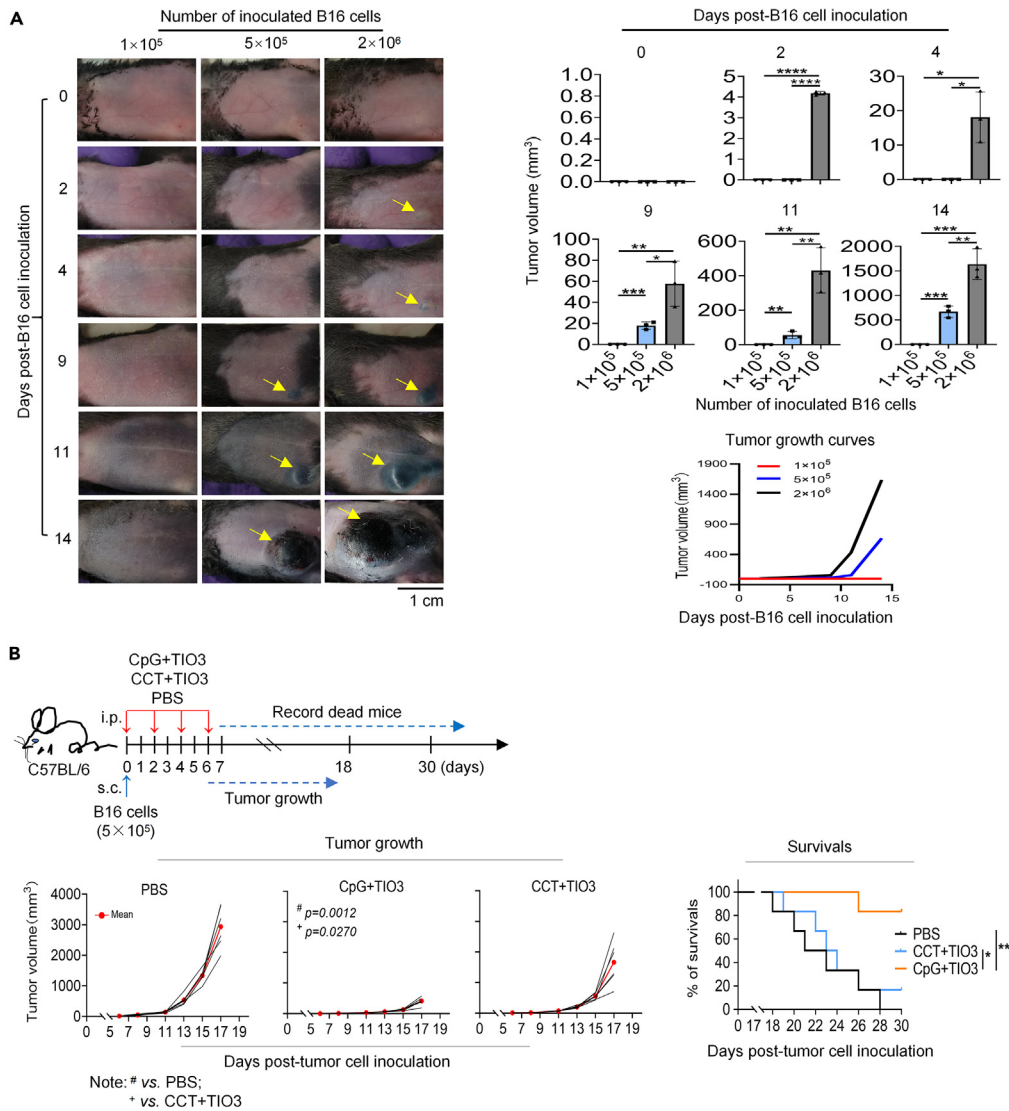
Figure 6. The impact of systemically applied ODNs on the tumor growth and survival of model mice

(A) Determination of the inoculation number of B16 cells suitable for tumor growth inhibition experiments in subcutaneous tumor-bearing mice. There were 3 mice in each group.

(B) The experimental procedure of ODNs treatment and the curves of tumor growth and survival of tumor-bearing mice. There were 6 mice in each group. Data are from one experiment. Data are expressed as mean $\pm$ SD, $*p < 0.05$, $**p < 0.01$, $***p < 0.001$, $****p < 0.0001$.

increased, while Ly6G$^+$ neutrophils, CD8$^+$ T cells, and NK cells were significantly reduced. Although the proportion of Ly6G$^+$ cells was still consistent with that in the control group, their number was reduced from about 860,000 to 710,000, while the proportion and number of CD8$^+$ and NK cells were also significantly reduced. Looking at the GFP$^+$ immune cells in the nodules, the number of all three types of GFP$^+$ immune cells was obviously reduced compared to that of the control group (Figure 7E). These results suggest that reducing the recruitment of neutrophils to early tumor nodules can simultaneously reduce the recruitment and activation of CD8$^+$ T cells and NK cells, indicating the direct or indirect anti-tumor activity of trogocytic neutrophils.

DISCUSSION

In this study, we investigated trogocytic neutrophils in early tumor nodules induced by s.c. inoculated B16 melanoma cells and their association with the establishment of an anti-tumor immune microenvironment and tumor growth inhibition.

The mouse s.c. transplanted tumor model is a widely used research platform.[43–45] However, previous studies have overlooked the presence of neutrophil-rich subcutaneous early tumor nodules induced by inoculated tumor cells. In this study, we found that these early tumor nodules were clearly visible at 24 h after the tumor cells were inoculated. In the tumor nodule cells, neutrophils accounted for about 65% and
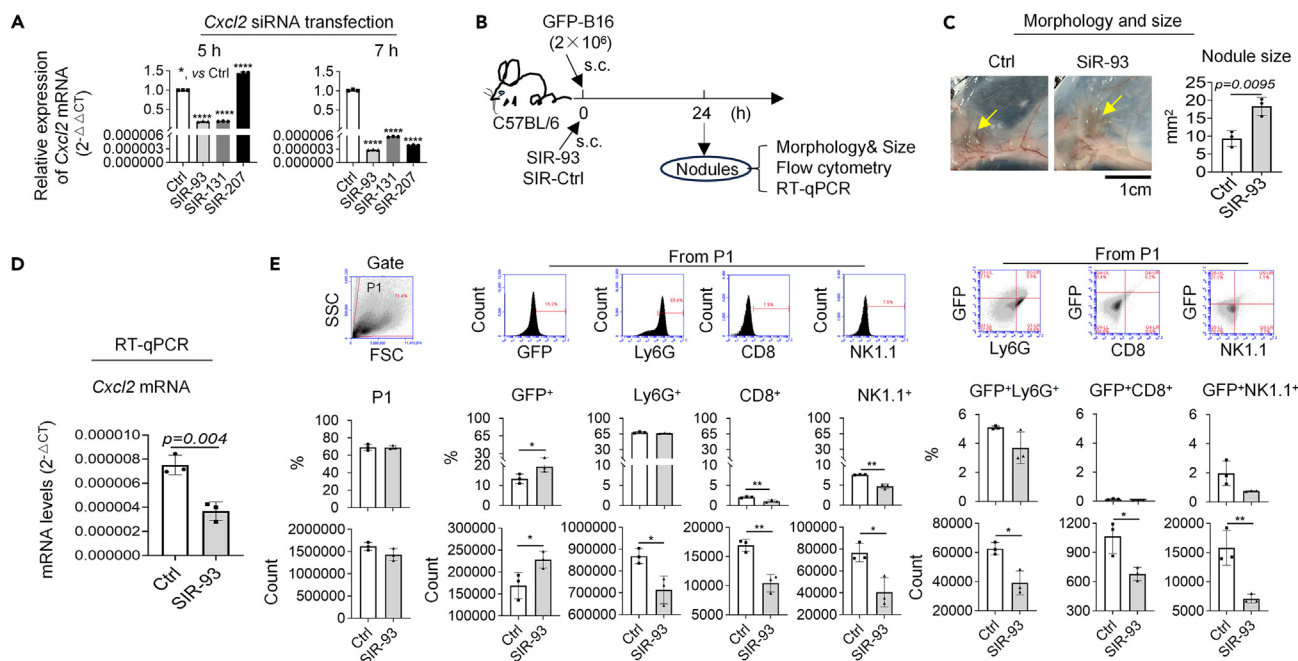
Figure 7. RNAi of *Cxcl2* and its effects on *Cxcl2* mRNA expression, neutrophil recruitment, and cell composition in tumor nodules

(A) Identification of three *Cxcl2* siRNAs on B16 cells by RT-qPCR.

(B) Experimental procedure of *Cxcl2* siRNA application in mice.

(C) The morphology and size of tumor nodules.

(D) *Cxcl2* mRNA levels in tumor nodules detected by RT-qPCR.

(E) The percentage and number of different cells in tumor nodules detected by flow cytometry. Each *in vitro* experiment represents one out of three. There are three mice in each group of the *in vivo* experiments. Data are from one of two experiments. Data are expressed as mean $\pm$ SD, $*p < 0.05$, $**p < 0.01$, $****p < 0.0001$.

this proportion remained constant during subsequent observation periods (as short as 6 h and as long as 36 h), in which some of neutrophils attacked the tumor cells by trogocytosis. By comparing the difference in tumor cell size in Figures 2E, 2F, and 3B, it can be seen that neutrophils can not only attack tumor cells by trogocytosis but also engulf the microparticles released by tumor cells because tumor cell-derived microparticles can also carry fluorescence signals.[46] We preferred B16 melanoma cells as the cell line to establish subcutaneous tumor model, mainly based on two considerations that are as follows. First, B16 cells are tumor cells of skin origin, and subcutaneous B16 cell tumor model belongs to orthotopic transplantation tumor, so the growth of tumor cells is closer to the natural growth environment. Second, B16 cells have melanin, which is advantageous in tumor nodule separation. Although this transplanted tumor model is very different from natural tumorigenesis, considering that this is, after all, an initial tumor model, we were very interested in this. For the phenomenon that subcutaneous inoculation of a few hundred tumor cells does not form tumors, we suspect that the small number of transplanted tumor cells that spread as rapidly as the injected medium after inoculation are destroyed before they aggregate to grow into tumors, and therefore they have no ability to recruit neutrophils. As for why neutrophils arrive at the site of tumor cell inoculation, according to our experimental results, chemokines, such as CXCL2, produced by B16 melanoma cells, may be the first driving force. Chemokines produced by CD45$^+$ leukocytes (especially recruited neutrophils) in nodules may provide positive feedback driving force for subsequent recruitment of neutrophils. This is also supported by literatures that both B16F10 melanoma cells[47] and resident macrophages[48] can express the chemokine CXCL1/2 that can recruit neutrophils. As for why neutrophils attack tumor cells in early tumor nodules by trogocytosis, we do not know, but we can speculate that this should be an active behavior of neutrophils to destroy invaders. In our experience, tumor formation is difficult when the number of inoculated tumor cells is insufficient. Thus, the trogocytosis of neutrophils recruited to the site of tumor cell inoculation may be one of several ways to limit the initial formation of tumors. As for why the proportion of neutrophils in early tumor nodules remains constant over time, there may be two reasons of long lifespan and continuous recruitment. Our *in vitro* experiments show that the lifespan of neutrophils is not extended, and trogocytic ability of neutrophils seems to be domesticated by tumor cells. We co-cultured BMCs with B16 cells (Figure S1A) and found that there was no deference between the number of neutrophils in the BMC+B16 group and that in the BMC group at 1, 3, and 6 h during co-incubation. In addition, during co-incubation, the number of neutrophils remained unchanged at 1–3 h and then decreased at 6 h (Figure S1B). These results show that the lifespan of neutrophils in the co-cultured system does not change in the short term but changes over longer co-incubation. Furthermore, neutrophils weakened their killing ability under the domestication of tumor cells, which was also verified by our *in vitro* experiments. In the co-culture system of GFP-B16 cells and BMCs, the proportion of GFP$^+$Ly6G$^+$ neutrophils gradually decreased over time (Figure S1), which means fewer neutrophils gnawing on tumor cells. In a word, the inoculated tumor cells can both recruit neutrophils and domesticate the recruited

neutrophils in mice to transform them in a direction favorable to tumor growth. This suggests that early tumor nodules induced by inoculated tumor cells may indeed be a potentially valuable platform for studying tumor-associated neutrophils from different aspects of natural tumorigenesis.

Few reports have investigated whether neutrophils with phagocytic/gnawing capabilities actually help limit tumor development at the initial stage. Most studies have focused on the dual roles of neutrophils in solid tumors, either promoting[14,49–52] or inhibiting[18–20,26,53] tumor development in the tumor microenvironment. This is related to the lack of suitable models because naturally occurring tumors in mice and humans are a chronic disease, and even the very small nodule seen by imaging examination is actually not the initial stage of the tumor. Our study found that neutrophils are the first responder to arrive locally during the initial stage of s.c. transplanted tumor in mice, and some of these neutrophils can kill tumor cells through trogocytosis. In the tumor-initiation stage, that is, when the tumor microenvironment has not yet been formed, the systematic application of immunomodulators, such as TLR9 agonist CpG ODN combined with TGF-β2 inhibitor TIO3 (CpG+TIO3), will increase the proportion of total neutrophils and trogocytic neutrophils in early tumor nodules. Meanwhile, the proportion of CD8$^+$ T cells, NK cells, IFNγ$^+$CD8$^+$ cells, and IFNγ$^+$NK1.1$^+$ cells is also increased. This is related to TLR9 activation, as there is no such phenomenon with the TLR9 inhibitor CCT ODN. In addition, the genomic DNA in NETs is also known to activate TLR9,[5,8] and trogocytic neutrophils may activate TLR9 in a NETs-dependent manner. The activation of TLR9 signals can induce the production of various chemokines including chemotactic lymphocyte chemokines such as CXCL9-13, CCL16, CCL17, CCL19, and CCL21.[54–58] We used siRNA targeting *Cxcl2* mRNA to reduce the recruitment of neutrophils in tumor nodules, which also reduced the mRNA expression of chemotactic lymphocyte chemokines such as CXCL10, CXCL13, and CCL19 in the nodules (Figure S2). Combined with the result in Figure 7E in which the reduction of neutrophil recruitment is along with the reduction of CD8$^+$ T cells and NK cells, this result suggests that chemokines produced by increased neutrophils and trogocytic neutrophils in tumor nodules play a role in inducing the arrival of CD8$^+$ T cells and NK cells. In addition, this seems to indicate that the increase of trogocytic neutrophils in early tumor nodules is linked to the formation of an anti-tumor microenvironment. Although the mechanism of the association between trogocytic neutrophils and the anti-tumor microenvironment is still unclear, we found that CpG+TIO3 increased the CD86 levels on neutrophils in early tumor nodules in addition to the increase of trogocytic neutrophils, which at least suggests that these neutrophils are also capable of activating CD8$^+$ T cells by presenting tumor antigens. Subsequent experiments of tumor growth inhibition also confirmed this because CpG+TIO3 can significantly inhibit tumor growth and prolong the survival of model mice. One of our previous studies has shown that the intraperitoneal administration of CpG+TIO3 in subcutaneous lung cancer model mice can elevate the levels of IFN-γ expression and the ratios of NK cells and CD8$^+$ T cells in tumors and promote the activation of DCs in the tumor microenvironment.[41] However, in that study, neutrophils were not looked at, and the acquisition time of tumor was relatively late, at 13 days after tumor cell inoculation, which was already tumor tissue compared to the 24 h tumor nodules in this study. We found in this study that there are no DCs in this 24 h early tumor nodule, suggesting that this initial activation of T cells and NK cells came from neutrophils, particularly trogocytic neutrophils. We used siRNA targeting to *Cxcl2* mRNA (a chemokine for recruiting neutrophils) to downregulate neutrophil recruitment in tumor nodules and also demonstrated that the activation of CD8$^+$ T cells and NK cells in early tumor nodules came from neutrophils that arrived early in tumor nodules. Whether this relationship between neutrophils and these two types of immune cells with the ability to kill tumor cells remains true during tumor development needs to be further demonstrated in subsequent studies.

In conclusion, from our results, we may venture to speculate that when tumor cells (or mutated cells) appear in a particular part of the body, neutrophils are the first immune cells to arrive at that location and try to eliminate them by trogocytosis or activating other immune cells. If the body's immune system is properly active or activated at this time, it will be conducive to neutrophils to play a trogocytic role. If this process is very successful, the tumor cells are killed in the cradle, and the tumor does not occur.

Limitations of the study

The transplanted mouse tumor models we used are not naturally occurring tumors, and the conclusions we obtained are not representative of natural tumorigenesis. However, the presence of a large number of neutrophils in early tumor nodules prior to tumor formation in the model mice is indeed a useful platform to study tumor-associated neutrophils, thus providing valuable data for the timing and mode of immunotherapy in patients after tumor surgery.

STAR★METHODS

Detailed methods are provided in the online version of this paper and include the following:

- ○ Cell and cell culture
- ○ Oligodeoxynucleotides (ODNs)
- ○ Flow cytometry
- ○ Preparation of frozen sections and tissue paraffin sections
- ○ Hematoxylin and eosin (H&E) staining
- ○ Immunofluorescence assay
- ○ Immunohistochemical staining
- ○ Establishment of *in vitro* experiment system
- ○ RNA interference assay
- ○ Total RNA isolation and RT-qPCR
- ● QUANTIFICATION AND STATISTICAL ANALYSIS

REFERENCES

1. Singhal, A., and Kumar, S. (2022). Neutrophil and remnant clearance in immunity and inflammation. Immunology *165*, 22–43. https://doi.org/10.1111/imm.13423.

2. Hidalgo, A., Libby, P., Soehnlein, O., Aramburu, I.V., Papayannopoulos, V., and Silvestre-Roig, C. (2022). Neutrophil extracellular traps: from physiology to pathology. Cardiovasc. Res. *118*, 2737–2753. https://doi.org/10.1093/cvr/cvab329.

3. Burn, G.L., Foti, A., Marsman, G., Patel, D.F., and Zychlinsky, A. (2021). The Neutrophil. Immunity *54*, 1377–1391. https://doi.org/10.1016/j.immuni.2021.06.006.

4. Ley, K., Hoffman, H.M., Kubes, P., Cassatella, M.A., Zychlinsky, A., Hedrick, C.C., and Catz, S.D. (2018). Neutrophils: New insights and open questions. Sci. Immunol. *3*, eaat4579. https://doi.org/10.1126/sciimmunol.aat4579.

5. Sun, S., Duan, Z., Wang, X., Chu, C., Yang, C., Chen, F., Wang, D., Wang, C., Li, Q., and Ding, W. (2021). Neutrophil extracellular traps impair intestinal barrier functions in sepsis by regulating TLR9-mediated endoplasmic reticulum stress pathway. Cell Death Dis. *12*, 606. https://doi.org/10.1038/s41419-021-03896-1.

6. Liu, D., Yang, P., Gao, M., Yu, T., Shi, Y., Zhang, M., Yao, M., Liu, Y., and Zhang, X. (2019). NLRP3 activation induced by neutrophil extracellular traps sustains inflammatory response in the diabetic wound. Clin. Sci. *133*, 565–582. https://doi.org/10.1042/CS20180600.

7. Huang, H., Tohme, S., Al-Khafaji, A.B., Tai, S., Loughran, P., Chen, L., Wang, S., Kim, J., Billiar, T., Wang, Y., and Tsung, A. (2015). Damage-associated molecular pattern-activated neutrophil extracellular trap exacerbates sterile inflammatory liver injury. Hepatology *62*, 600–614. https://doi.org/10.1002/hep.27841.

8. Liu, L., Mao, Y., Xu, B., Zhang, X., Fang, C., Ma, Y., Men, K., Qi, X., Yi, T., Wei, Y., and Wei, X. (2019). Induction of neutrophil extracellular traps during tissue injury: Involvement of STING and Toll-like receptor 9 pathways. Cell Prolif. *52*, e12579. https://doi.org/10.1111/cpr.12579.

9. Kou, M., Lu, W., Zhu, M., Qu, K., Wang, L., and Yu, Y. (2023). Massively recruited sTLR9(+) neutrophils in rapidly formed nodules at the site of tumor cell inoculation and their contribution to a pro-tumor microenvironment. Cancer Immunol. Immunother. *72*, 2671–2686. https://doi.org/10.1007/s00262-023-03451-1.

10. Lämmermann, T., Afonso, P.V., Angermann, B.R., Wang, J.M., Kastenmüller, W., Parent, C.A., and Germain, R.N. (2013). Neutrophil swarms require LTB4 and integrins at sites of cell death in vivo. Nature *498*, 371–375. https://doi.org/10.1038/nature12175.

11. Yoo, S.K., Starnes, T.W., Deng, Q., and Huttenlocher, A. (2011). Lyn is a redox sensor that mediates leukocyte wound attraction in vivo. Nature *480*, 109–112. https://doi.org/10.1038/nature10632.

12. Carnevale, S., Di Ceglie, I., Grieco, G., Rigatelli, A., Bonavita, E., and Jaillon, S. (2023). Neutrophil diversity in inflammation and cancer. Front. Immunol. *14*, 1180810. https://doi.org/10.3389/fimmu.2023.1180810.

13. Jaillon, S., Ponzetta, A., Di Mitri, D., Santoni, A., Bonecchi, R., and Mantovani, A. (2020). Neutrophil diversity and plasticity in tumour progression and therapy. Nat. Rev. Cancer *20*, 485–503. https://doi.org/10.1038/s41568-020-0281-y.

14. Zhu, Y.P., Padgett, L., Dinh, H.Q., Marcovecchio, P., Blatchley, A., Wu, R., Ehinger, E., Kim, C., Mikulski, Z., Seumois, G., et al. (2018). Identification of an Early Unipotent Neutrophil Progenitor with Pro-tumoral Activity in Mouse and Human Bone Marrow. Cell Rep. 24, 2329–2341.e8. https://doi.org/10.1016/j.celrep.2018.07.097.

15. Spiegel, A., Brooks, M.W., Houshyar, S., Reinhardt, F., Ardolino, M., Fessler, E., Chen, M.B., Krall, J.A., DeCock, J., Zervantonakis, I.K., et al. (2016). Neutrophils Suppress Intraluminal NK Cell-Mediated Tumor Cell Clearance and Enhance Extravasation of Disseminated Carcinoma Cells. Cancer Discov. 6, 630–649. https://doi.org/10.1158/2159-8290.CD-15-1157.

16. Casbon, A.J., Reynaud, D., Park, C., Khuc, E., Gan, D.D., Schepers, K., Passegué, E., and Werb, Z. (2015). Invasive breast cancer reprograms early myeloid differentiation in the bone marrow to generate immunosuppressive neutrophils. Proc. Natl. Acad. Sci. USA 112, E566–E575. https://doi.org/10.1073/pnas.1424927112.

17. Zhang, Y., Chandra, V., Riquelme Sanchez, E., Dutta, P., Quesada, P.R., Rakoski, A., Zoltan, M., Arora, N., Baydogan, S., Horne, W., et al. (2020). Interleukin-17-induced neutrophil extracellular traps mediate resistance to checkpoint blockade in pancreatic cancer. J. Exp. Med. 217, e20190354. https://doi.org/10.1084/jem.20190354.

18. Hirschhorn, D., Budhu, S., Schröder, D., Kraehenbuehl, L., Flammar, A.L., Chow, A., Schulze, I., Schad, S., Ricca, J., Gasmi, B., et al. (2021). T Cell Immunotherapies Trigger Neutrophil Activation To Eliminate Tumor Antigen Escape Variants. J. Immunother. Cancer 9, A108. https://doi.org/10.1136/jitc-2021-SITC2021.099.

19. Cui, C., Chakraborty, K., Tang, X.A., Zhou, G., Schoenfelt, K.Q., Becker, K.M., Hoffman, A., Chang, Y.F., Blank, A., Reardon, C.A., et al. (2021). Neutrophil elastase selectively kills cancer cells and attenuates tumorigenesis. Cell 184, 3163–3177.e21. https://doi.org/10.1016/j.cell.2021.04.016.

20. Gershkovitz, M., Caspi, Y., Fainsod-Levi, T., Katz, B., Michaeli, J., Khawaled, S., Lev, S., Polyansky, L., Shaul, M.E., Sionov, R.V., et al. (2018). TRPM2 Mediates Neutrophil Killing of Disseminated Tumor Cells. Cancer Res. 78, 2680–2690. https://doi.org/10.1158/0008-5472.CAN-17-3614.

21. García-Navas, R., Gajate, C., and Mollinedo, F. (2021). Neutrophils drive endoplasmic reticulum stress-mediated apoptosis in cancer cells through arginase-1 release. Sci. Rep. 11, 12574. https://doi.org/10.1038/s41598-021-91947-0.

22. Kuwabara, W.M.T., Andrade-Silva, J., Pereira, J.N.B., Scialfa, J.H., and Cipolla-Neto, J. (2019). Neutrophil activation causes tumor regression in Walker 256 tumor-bearing rats. Sci. Rep. 9, 16524. https://doi.org/10.1038/s41598-019-52956-2.

23. Sionov, R.V., Fainsod-Levi, T., Zelter, T., Polyansky, L., Pham, C.T., and Granot, Z. (2019). Neutrophil Cathepsin G and Tumor Cell RAGE Facilitate Neutrophil Anti-Tumor Cytotoxicity. OncoImmunology 8, e1624129. https://doi.org/10.1080/2162402X.2019.1624129.

24. Hirschhorn, D., Budhu, S., Kraehenbuehl, L., Gigoux, M., Schröder, D., Chow, A., Ricca, J.M., Gasmi, B., De Henau, O., Mangarin, L.M.B., et al. (2023). T cell immunotherapies engage neutrophils to eliminate tumor antigen escape variants. Cell 186, 1432–1447.e17. https://doi.org/10.1016/j.cell.2023.03.007.

25. Gungabeesoon, J., Gort-Freitas, N.A., Kiss, M., Bolli, E., Messemaker, M., Siwicki, M., Hicham, M., Bill, R., Koch, P., Cianciaruso, C., et al. (2023). A neutrophil response linked to tumor control in immunotherapy. Cell 186, 1448–1464.e20. https://doi.org/10.1016/j.cell.2023.02.032.

26. Blaisdell, A., Crequer, A., Columbus, D., Daikoku, T., Mittal, K., Dey, S.K., and Erlebacher, A. (2015). Neutrophils Oppose Uterine Epithelial Carcinogenesis via Debridement of Hypoxic Tumor Cells. Cancer Cell 28, 785–799. https://doi.org/10.1016/j.ccell.2015.11.005.

27. Eruslanov, E.B., Bhojnagarwala, P.S., Quatromoni, J.G., Stephen, T.L., Ranganathan, A., Deshpande, C., Akimova, T., Vachani, A., Litzky, L., Hancock, W.W., et al. (2014). Tumor-associated neutrophils stimulate T cell responses in early-stage human lung cancer. J. Clin. Invest. 124, 5466–5480. https://doi.org/10.1172/JCI77053.

28. Singhal, S., Bhojnagarwala, P.S., O'Brien, S., Moon, E.K., Garfall, A.L., Rao, A.S., Quatromoni, J.G., Stephen, T.L., Litzky, L., Deshpande, C., et al. (2016). Origin and Role of a Subset of Tumor-Associated Neutrophils with Antigen-Presenting Cell Features in Early-Stage Human Lung Cancer. Cancer Cell 30, 120–135. https://doi.org/10.1016/j.ccell.2016.06.001.

29. Mahiddine, K., Blaisdell, A., Ma, S., Créquer-Grandhomme, A., Lowell, C.A., and Erlebacher, A. (2020). Relief of tumor hypoxia unleashes the tumoricidal potential of neutrophils. J. Clin. Invest. 130, 389–403. https://doi.org/10.1172/JCI130952.

30. Finisguerra, V., Di Conza, G., Di Matteo, M., Serneels, J., Costa, S., Thompson, A.A.R., Wauters, E., Walmsley, S., Prenen, H., Granot, Z., et al. (2015). MET is required for the recruitment of anti-tumoural neutrophils. Nature 522, 349–353. https://doi.org/10.1038/nature14407.

31. Kalafati, L., Kourtzelis, I., Schulte-Schrepping, J., Li, X., Hatzioannou, A., Grinenko, T., Hagag, E., Sinha, A., Has, C., Dietz, S., et al. (2020). Innate Immune Training of Granulopoiesis Promotes Anti-tumor Activity. Cell 183, 771–785.e12. https://doi.org/10.1016/j.cell.2020.09.058.

32. Matlung, H.L., Babes, L., Zhao, X.W., van Houdt, M., Treffers, L.W., van Rees, D.J., Franke, K., Schornagel, K., Verkuijlen, P., Janssen, H., et al. (2018). Neutrophils Kill Antibody-Opsonized Cancer Cells by Trogoptosis. Cell Rep. 23, 3946–3959.e6. https://doi.org/10.1016/j.celrep.2018.05.082.

33. Tabiasco, J., Espinosa, E., Hudrisier, D., Joly, E., Fournie, J.J., and Vercellone, A. (2002). Active trans-synaptic capture of membrane fragments by natural killer cells. Eur. J. Immunol. 32, 1502–1508. https://doi.org/10.1002/1521-4141(200205)32:5<1502::AID-IMMU1502>3.0.CO;2-Y.

34. Joly, E., and Hudrisier, D. (2003). What is trogocytosis and what is its purpose? Nat. Immunol. 4, 815. https://doi.org/10.1038/ni0903-815.

35. Pagliano, O., Morrison, R.M., Chauvin, J.M., Banerjee, H., Davar, D., Ding, Q., Tanegashima, T., Gao, W., Chakka, S.R., DeBlasio, R., et al. (2022). Tim-3 mediates T cell trogocytosis to limit antitumor immunity. J. Clin. Invest. 132, e152864. https://doi.org/10.1172/JCI152864.

36. Velmurugan, R., Challa, D.K., Ram, S., Ober, R.J., and Ward, E.S. (2016). Macrophage-Mediated Trogocytosis Leads to Death of Antibody-Opsonized Tumor Cells. Mol. Cancer Therapeut. 15, 1879–1889. https://doi.org/10.1158/1535-7163.MCT-15-0335.

37. Shin, J.H., Jeong, J., Maher, S.E., Lee, H.W., Lim, J., and Bothwell, A.L.M. (2021). Colon cancer cells acquire immune regulatory molecules from tumor-infiltrating lymphocytes by trogocytosis. Proc. Natl. Acad. Sci. USA 118, e2110241118. https://doi.org/10.1073/pnas.2110241118.

38. Acharyya, S., Oskarsson, T., Vanharanta, S., Malladi, S., Kim, J., Morris, P.G., Manova-Todorova, K., Leversha, M., Hogg, N., Seshan, V.E., et al. (2012). A CXCL1 paracrine network links cancer chemoresistance and metastasis. Cell 150, 165–178. https://doi.org/10.1016/j.cell.2012.04.042.

39. Jablonska, J., Wu, C.F., Andzinski, L., Leschner, S., and Weiss, S. (2014). CXCR2-mediated tumor-associated neutrophil recruitment is regulated by IFN-beta. Int. J. Cancer 134, 1346–1358. https://doi.org/10.1002/ijc.28551.

40. López-Lago, M.A., Posner, S., Thodima, V.J., Molina, A.M., Motzer, R.J., and Chaganti, R.S.K. (2013). Neutrophil chemokines secreted by tumor cells mount a lung antimetastatic response during renal cell carcinoma progression. Oncogene 32, 1752–1760. https://doi.org/10.1038/onc.2012.201.

41. Yao, Y., Li, J., Qu, K., Wang, Y., Wang, Z., Lu, W., Yu, Y., and Wang, L. (2023). Immunotherapy for lung cancer combining the oligodeoxynucleotides of TLR9 agonist and TGF-beta2 inhibitor. Cancer Immunol. Immunother. 72, 1103–1120. https://doi.org/10.1007/s00262-022-03315-0.

42. Silvestre-Roig, C., Fridlender, Z.G., Glogauer, M., and Scapini, P. (2019). Neutrophil Diversity in Health and Disease. Trends Immunol. 40, 565–583. https://doi.org/10.1016/j.it.2019.04.012.

43. Scatozza, F., Moschella, F., D'Arcangelo, D., Rossi, S., Tabolacci, C., Giampietri, C., Proietti, E., Facchiano, F., and Facchiano, A. (2020). Nicotinamide inhibits melanoma in vitro and in vivo. J. Exp. Clin. Cancer Res. 39, 211. https://doi.org/10.1186/s13046-020-01719-3.

44. Tikoo, S., Jain, R., Tomasetig, F., On, K., Martinez, B., Heu, C., Stehle, D., Obeidy, P., Guo, D., Vincent, J.N., et al. (2021). Amelanotic B16-F10 Melanoma Compatible with Advanced Three-Dimensional Imaging Modalities. J. Invest. Dermatol. 141, 2090–2094.e6. https://doi.org/10.1016/j.jid.2021.01.025.

45. Uurasmaa, T.M., Streng, T., Alkio, M., Karikoski, M., Heinonen, I., and Anttila, K. (2022). Subcutaneous B16 melanoma impairs intrinsic pressure generation and relaxation of the heart, which are not restored by short-term voluntary exercise in mice. Am. J. Physiol. Heart Circ. Physiol. 322, H1044–H1056. https://doi.org/10.1152/ajpheart.00586.2021.

46. Yang, F., Liu, S., Liu, X., Liu, L., Luo, M., Qi, S., Xu, G., Qiao, S., Lv, X., Li, X., et al. (2016). In Vivo Visualization of Tumor Antigen-containing Microparticles Generated in Fluorescent-protein-elicited Immunity. Theranostics 6, 1453–1466. https://doi.org/10.7150/thno.14145.

47. Shi, H., Han, X., Sun, Y., Shang, C., Wei, M., Ba, X., and Zeng, X. (2018). Chemokine (C-X-C motif) ligand 1 and CXCL2 produced by

tumor promote the generation of monocytic myeloid-derived suppressor cells. Cancer Sci. *109*, 3826–3839. https://doi.org/10.1111/cas.13809.

48. De Filippo, K., Dudeck, A., Hasenberg, M., Nye, E., van Rooijen, N., Hartmann, K., Gunzer, M., Roers, A., and Hogg, N. (2013). Mast cell and macrophage chemokines CXCL1/CXCL2 control the early stage of neutrophil recruitment during tissue inflammation. Blood *121*, 4930–4937. https://doi.org/10.1182/blood-2013-02-486217.

49. Demers, M., Wong, S.L., Martinod, K., Gallant, M., Cabral, J.E., Wang, Y., and Wagner, D.D. (2016). Priming of neutrophils toward NETosis promotes tumor growth. OncoImmunology *5*, e1134073. https://doi.org/10.1080/2162402X.2015.1134073.

50. Engblom, C., Pfirschke, C., Zilionis, R., Da Silva Martins, J., Bos, S.A., Courties, G., Rickelt, S., Severe, N., Baryawno, N., Faget, J., et al. (2017). Osteoblasts remotely supply lung tumors with cancer-promoting SiglecF(high) neutrophils. Science *358*, eaal5081. https://doi.org/10.1126/science.aal5081.

51. Houghton, A.M., Rzymkiewicz, D.M., Ji, H., Gregory, A.D., Egea, E.E., Metz, H.E., Stolz, D.B., Land, S.R., Marconcini, L.A., Kliment, C.R., et al. (2010). Neutrophil elastase-mediated degradation of IRS-1 accelerates lung tumor growth. Nat. Med. *16*, 219–223. https://doi.org/10.1038/nm.2084.

52. Coffelt, S.B., Kersten, K., Doornebal, C.W., Weiden, J., Vrijland, K., Hau, C.S., Verstegen, N.J.M., Ciampricotti, M., Hawinkels, L.J.A.C., Jonkers, J., and de Visser, K.E. (2015). IL-17-

producing gammadelta T cells and neutrophils conspire to promote breast cancer metastasis. Nature *522*, 345–348. https://doi.org/10.1038/nature14282.

53. Martinez Sanz, P., van Rees, D.J., van Zogchel, L.M.J., Klein, B., Bouti, P., Olsman, H., Schornagel, K., Kok, I., Sunak, A., Leeuwenburg, K., et al. (2021). G-CSF as a suitable alternative to GM-CSF to boost dinutuximab-mediated neutrophil cytotoxicity in neuroblastoma treatment. J. Immunother. Cancer *9*, e002259. https://doi.org/10.1136/jitc-2020-002259.

54. Wendel, M., Galani, I.E., Suri-Payer, E., and Cerwenka, A. (2008). Natural killer cell accumulation in tumors is dependent on IFN-gamma and CXCR3 ligands. Cancer Res. *68*, 8437–8445. https://doi.org/10.1158/0008-5472.CAN-08-1440.

55. Hensbergen, P.J., Wijnands, P.G.J.T.B., Schreurs, M.W.J., Scheper, R.J., Willemze, R., and Tensen, C.P. (2005). The CXCR3 targeting chemokine CXCL11 has potent antitumor activity in vivo involving attraction of CD8+ T lymphocytes but not inhibition of angiogenesis. J. Immunother. *28*, 343–351. https://doi.org/10.1097/01.cji.0000165355.26795.27.

56. Singh, R., Lillard, J.W., Jr., and Singh, S. (2011). Chemokines: key players in cancer progression and metastasis. Front. Biosci. *3*, 1569–1582. https://doi.org/10.2741/246.

57. Cremonesi, E., Governa, V., Garzon, J.F.G., Mele, V., Amicarella, F., Muraro, M.G., Trella, E., Galati-Fournier, V., Oertli, D., Däster, S.R., et al. (2018). Gut microbiota modulate T cell trafficking into human colorectal cancer. Gut

67, 1984–1994. https://doi.org/10.1136/gutjnl-2016-313498.

58. Yagawa, Y., Robertson-Tessi, M., Zhou, S.L., Anderson, A.R.A., Mulé, J.J., and Mailloux, A.W. (2017). Systematic Screening of Chemokines to Identify Candidates to Model and Create Ectopic Lymph Node Structures for Cancer Immunotherapy. Sci. Rep. *7*, 15996. https://doi.org/10.1038/s41598-017-15924-2.

59. Li, D., Li, H., Zhang, P., Wu, X., Wei, H., Wang, L., Wan, M., Deng, P., Zhang, Y., Wang, J., et al. (2006). Heat shock fusion protein induces both specific and nonspecific anti-tumor immunity. Eur. J. Immunol. *36*, 1324–1336. https://doi.org/10.1002/eji.200535490.

60. Chen, Y., Su, X., Wang, L., and Yu, Y. (2008). Establishment of B16 cell line expressing MUC1 VNTR by in vivo passage and sorting. Immunoidgical Journal *24*, 1–8. https://doi.org/10.13431/j.cnki.immunol.j.20080001.

61. Zhao, P., Yang, L., Li, X., Lu, W., Lu, F., Wang, S., Wang, Y., Hua, L., Cui, C., Dong, B., et al. (2020). Rae1 drives NKG2D binding-dependent tumor development in mice by activating mTOR and STAT3 pathways in tumor cells. Cancer Sci. *111*, 2234–2247. https://doi.org/10.1111/cas.14434.

62. Tu, L., Sun, X., Yang, L., Zhang, T., Zhang, X., Li, X., Dong, B., Liu, Y., Yang, M., Wang, L., and Yu, Y. (2020). TGF-beta2 interfering oligonucleotides used as adjuvants for microbial vaccines. J. Leukoc. Biol. *108*, 1673–1692. https://doi.org/10.1002/JLB.5A0420-491R.

STAR★METHODS

KEY RESOURCES TABLE

REAGENT or RESOURCE	SOURCE	IDENTIFIER
Antibodies		
Rat monoclonal anti-Mouse Ly6G,	BD	Cat#551461; RRID:AB_394208
Rat monoclonal anti-Mouse F4/80	BD	Cat#565410; RRID:AB_2687527
Rat monoclonal anti-Mouse CD45	BD	Cat#559864; RRID:AB_398672
Mouse monoclonal anti-Mouse NK1.1	BD	Cat#550627; RRID:AB_398463
Mouse monoclonal anti-Mouse NK1.1	BD	Cat#553164; RRID:AB_394676
Rat monoclonal anti-Mouse CD8a	BD	Cat#553033; RRID:AB_394571
Rat monoclonal anti-Mouse CD19	BD	Cat#557399; RRID:AB_396682
Hamster monoclonal anti-Mouse CD11c	BD	Cat#553801; RRID:AB_395060
Rat monoclonal anti-Mouse CD86	BD	Cat#558703; RRID:AB_2075114
Hamster monoclonal anti-Mouse CD3e	BD	Cat#553064; RRID:AB_394597
Rat monoclonal anti-Mouse IFN-γ	Thermo Fisher Scientific	Cat#17-7311-82; RRID:AB_469504
Rabbit monoclonal anti-mouse CXCL2	Abcam	Cat#ab25130; RRID:AB_448642
Goat polyclonal Anti-Rabbit IgG (H+L)	Proteintech	Cat#SA00003-2; RRID:AB_2890897
Mouse monoclonal anti-Mouse NK1.1	Biolegend	Cat#108701; RRID:AB_313388
Goat polyclonal Anti-mouse IgG (H+L)	Absin	Cat#abs20001; RRID:AB_2716555
Chemicals, peptides, and recombinant proteins		
7-AAD Viability Staining Solution	Yesen	Cat#40745ES64
QuickBlock™ Blocking Buffer for Immunol Staining	Beyotime	Cat#P0260
Critical commercial assays		
DAB Horseradish Peroxidase Color Development Kit	Beyotime	Cat#P0202
2×ES Reaction Mix and EasyScript®RT/RI Enzyme Mix	TransGen Biotech	Cat#AE301-02
PerfectStart® Green qPCR SuperMix	TransGen Biotech	Cat#AQ601
Experimental models: Cell lines		
Mouse: GFP-B16 cells	Li, D et al.,[59] Chen, Y et al.[60]	N/A
Mouse: B16 cells	Chen, Y et al.[60]	N/A
Mouse: GFP-GL261 cells	Zhao, P et al.[61]	N/A
Experimental models: Organisms/strains		
Mouse: Female C57BL/6 mice	Yisi Laboratory Animal Technology Co., Ltd.	https://www.ccyskj.cn/
Oligonucleotides		
TLR9 agonist CpG ODN	Yao et al.[41]	N/A
TLR9 inhibitor CCT ODN	Yao et al.[41]	N/A
TGF-β2 ASO TIO3	Yao et al.,[41] Tu et al.[62]	N/A
siRNA to Mus musculus *Cxcl2* # SIR-93: 5′-CAGUGAACUGCGCUGUCAATT-3′	This paper	N/A
siRNA to Mus musculus *Cxcl2* # SIR-131: 5′-GGGUUGACUUCAAGAACAUTT-3′	This paper	N/A
siRNA to Mus musculus *Cxcl2* # SIR-207: 5′-CACUCUCAAGGGCGGUCAATT-3′	This paper	N/A
siRNA to Mus musculus *Cxcl2* # SIR-Ctrl: 5′-UUCUCCGAACGUGUCACGUTT-3′	This paper	N/A

Continued

REAGENT or RESOURCE	SOURCE	IDENTIFIER
Primer to Mus musculus *Cxcl2* Forward: 5′-GCGCCCAGACAGAAGTCATA-3′	This paper	N/A
Primer to Mus musculus *Cxcl2* Reverse: 5′-CGAGGCACATCAGGTACGAT-3′	This paper	N/A
Primer to Mus musculus *β-actin* Forward: 5′-TGTGACGTTGACATCCGTAA-3′	This paper	N/A
Primer to Mus musculus*β-actin* Reverse: 5′-CCACCGATCCACACAGAGTA-3′	This paper	N/A
Primer to Mus musculus *Cxcl10* Forward: 5′-GTCCACGTGTTGAGATCATTGC-3′	This paper	N/A
Primer to Mus musculus *Cxcl10* Reverse: 5′-CTCTGTGTGGTCCATCCTTGG-3′	This paper	N/A
Primer to Mus musculus *Cxcl13* Forward: 5′-ATATGTGTGAATCCTCGTGCCA-3′	This paper	N/A
Primer to Mus musculus *Cxcl13* Reverse: 5′-GGGAGTTGAAGACAGACTTTTGC-3′	This paper	N/A
Primer to Mus musculus *Ccl19* Forward: 5′-CCTTCAGCCTGCTGGTTCTCT-3′	This paper	N/A
Primer to Mus musculus *Ccl19* Reverse: 5′-AGGCTTTCACGATGTTCCCAG-3′	This paper	N/A
Software and algorithms		
ImageJ	Schneider	https://imagej.net/ij/
Accuri C6	BD Biosciences	N/A
GraphPad Prism	GraphPad	https://www.graphpad.com/

RESOURCE AVAILABILITY

Lead contact

Further information and requests concerning the resources and reagents please send to the lead contact, Liying Wang (wangliy@jlu.edu.cn).

Materials availability

This study did not generate new reagents.

Data and code availability

- Data reported in this paper will be shared by the lead contact upon request.
- This paper does not report original code.
- Any additional information required to reanalyze the data reported in this paper is available from the lead contact upon request.

EXPERIMENTAL MODEL AND STUDY PARTICIPANT DETAILS

Mice and animal experiments

Female C57BL/6 mice aged 6-8-week-old were purchased from Yisi Laboratory Animal Technology Co., Ltd., in Changchun, China. The mice were raised under specific pathogen-free conditions at the Laboratory Animal Center of Jilin University and provided with free access to food and water.

To detect tumor nodules, 2×10^6 GFP-B16 cells were subcutaneously (s.c.) inoculated near the right hind leg on day 0. Mice were anesthetized and dissected at different times after the tumor cell inoculation to observe whether nodules formed subcutaneously at the site of inoculation. As a control, C57BL/6 mice were injected with culture medium in the same position and method as that of the mice were inoculated with tumor cells. Pictures were taken, and nodules or nodule-like tissues of mice inoculated with tumor cells and the corresponding tissue of mice injected with culture medium were isolated for subsequent study.

For treatment using oligodeoxynucleotide (ODN) combination, mice were s.c. inoculated with 2×10^6 GFP-B16 cells or B16 cells, and intraperitoneally injected with ODNs of TLR9 agonist CpG ODN or inhibitor CCT ODN in combination with TGF-β2 antisense ODN (ASO) TIO3 at

the same time. PBS injection was as control. The tumor nodules or nodule-like tissues were harvested from the mice treated by ODNs or PBS for further analysis at 24 h or different times after the inoculation.

To test therapeutic effect of systemically applied ODNs on tumor growth and the survival of mice, 5×10^5 B16 cells were subcutaneously inoculated on day 0. At the same time, CpG ODN+TIO3, CCT ODN+TIO3 was given intraperitoneally on day 0, 2, 4 and 6. PBS injection was as control. The tumor size was measured at different times after tumor cell inoculation and the death of mice was recorded (n = 6/group).

Preparation of tissue homogenates and cell suspensions

To prepare nodule or nodule-like tissue homogenates, harvested nodules or nodule-like tissues and then carefully removed the associated skin tissues, leaving only the nodules or subcutaneous tissue that enveloped tumor cells. Nodules or nodule-like tissues were put into RPMI 1640 medium/2% FBS and then ground with glass grinder to make homogenates. The homogenates were filtered with 300 mesh nylon cloth into 1.5 mL Eppendorf tube to obtain single-cell suspensions.

Study approval

The experiments were conducted in Institutes of Health Guide (revised in 1996, NIH Publication No. 80-23) and the guidelines for animal experiments at Jilin University, accordance with the Guidelines for the Care and Use of Laboratory Animals of the National Institutes of Health Guide, revised in 1996 (NIH Publication No. 80-23) and the guidelines for animal experiments at Jilin University. The Science and Technology Scientific Investigation Commission of Jilin Province, China, approved the experimental procedures, and the Ethics Committee of the College of Basic Medical Sciences, Jilin University, approved the mouse experiments.

METHOD DETAILS
Cell and cell culture

GFP-B16 cells were established by our team in the early years by stably transfecting GFP-MUC1 coding gene into murine B16 melanoma cells (B16 cells) of C57BL/6 origin.[59] In detailed, B16 cells were transfected with the pcDNA3-GFP-MUC1 VNTR plasmid encoding the human MUC1 VNTR peptide fused to GFP and then selected in medium containing G418 (500 μg/mL) (Sigma-Aldrich). The stable monoclonal transfected cells were verified by fluorescence microscopy and Western blotting analysis with anti-MUC1 mAb.[59] In order to maintain the stable expression of the transfected gene, GFP-B16 cells underwent subsequent *in vivo* passage and *in vitro* flow cytometry sorting.[59] Briefly, GFP-B16 cells were inoculated subcutaneously to develop into tumors in mice, and then the cells were separated from the tumors and sorted by flow cytometry according to whether they expressed GFP. After several rounds of this process of *in vivo* passage and *in vitro* sorting, B16 cells with stable expression of GFP (GFP-B16 cells) were finally obtained.[59] In this study, we selected the GFP positive characteristics of GFP-B16 cell line for the purpose of easily identifying and detecting tumor cells in the experiments. The GFP-B16 cells and B16 cells are currently stored in Department of Molecular Biology, College of Basic Medical Sciences, Jilin University.[60] GFP-GL261 cells are GFP-transfected cells established by our research group previously. Briefly, C57BL/6 mouse-derived GL261 glioma cells (American Type Culture Collection) are transfected stably with pcDNA3-GFP plasmids using Lipofectamine 3000 (Invitrogen, USA) and selected with G418 antibiotic (Millipore, USA).[61] To culture these cells, RPMI 1640 medium supplemented with 10% (v/v) Fetal Bovine Serum (FBS) and antibiotics (100 IU of penicillin/ml and 100 IU of streptomycin/ml) was used and maintained in a 5% CO_2 humidified incubator at 37°C.

Oligodeoxynucleotides (ODNs)

The single-stranded ODNs of the TLR9 agonist CpG ODN (CpG 5805), TLR9 inhibitor CCT ODN and TGF-β2 ASO TIO3 were used in mouse experiments.[41,62] All ODNs were synthesized, purified and fully phosphorothioate-modified by Takara Biotech (Dalian, China). The ODNs were diluted in PBS and no detectable endotoxin was detected by the LAL assay conducted by Associates of Cape Cod, Inc. (Massachusetts, USA).

Flow cytometry

Fluorescence-conjugated monoclonal antibodies of anti-Ly6G-PE (cat: 551461), F4/80-PE (cat: 565410), CD45-APC (cat: 559864), NK1.1-APC (cat: 550627), NK1.1-FITC (cat: 553164), CD8a-PE (cat: 553033), CD19-PE (cat: 557399), CD11c-FITC (cat: 553801), CD86-APC (cat: 558703) and CD3e-PE(cat: 553064) (BD Biosciences, NJ, USA) were used for cell surface staining in flow cytometry. IFN-γ-APC (Invitrogen, USA, Lot: 2410273), Rabbit anti-mouse CXCL2 antibody (Abcam, UK, cat: ab25130), FITC-conjugated Affinipure Goat Anti-Rabbit IgG(H+L) (Proteintech, USA, cat: SA00003-2) were used for intracellular staining in flow cytometry. The stained cells were detected and analyzed using BD-Accuri C6 flow cytometer (BD Biosciences, NJ, USA).

To analyze the cell composition ratio in tumor nodules, considering the limited channels in BD-Accuri C6 flow cytometer (BD Biosciences, NJ, USA) and the fact that GFP of GFP-B16 cells already occupied one channel, we set up four staining tubes for each sample from the nodule-like or nodule tissues, and used the GFP of GFP-B16 cells as quantitative standard and CD45-APC as relative reference in gating strategy between different staining tubes and accounted the percentage of various cells for each sample. For the tissue cell samples from the injection site of the culture medium, CD45-APC was used as the quantitative standard. The cells from each GFP-B16 nodule sample were added into four staining tubes and surface-stained with anti-Ly6G-PE and CD45-APC, anti-F4/80-PE and CD45-APC, anti-NK1.1-APC and CD3e-PE, and

anti-CD19-PE and CD45-APC, respectively. After staining in the staining buffer, the cells were washed once, suspended with PBS, and detected by flow cytometer.

Intracellular staining: After surface staining, the cells were fixed on ice with 4% paraformaldehyde for 15 min. After washing with PBS, 0.1% saponin was added and incubated on ice for 10 min. After washing with PBS, specific antibodies against target molecules were added. For intracellular staining of IFN-γ, APC-labeled anti-IFN-γ mAb was added and incubated on ice in dark for 30 min. Intracellular CXCL2 staining was performed by added rabbit anti-mouse CXCL2 mAb, followed by FITC-labeled sheep anti-rabbit IgG (H+L), and incubated on ice in dark for 30 min at each step. After washing with PBS, the cells were suspended in PBS/2%FBS, filtered with 300 mesh filter, and then placed on ice for use.

In order to exclude the influence of dead cells in flow cytometry results, we labeled the nodule cells with dead cell marker dye 7AAD (7-AAD Viability Staining Solution, Yesen, China, cat: 40745ES64) after surface staining with fluorescence-labeled antibodies, and then performed flow cytometry detection. When analyzing flow cytometry results, 7AAD⁻ cells were selected from P1 as a second-grade gating strategy to exclude the influence of dead cells on the results.

Preparation of frozen sections and tissue paraffin sections

To prepare frozen sections of tumor nodules, the tumor nodules were placed in an embedded plastic box, soaked in OCT embedding agent, and then carefully placed the plastic box in liquid nitrogen to make it quickly freeze into the block. The frozen embedding block was removed and placed on a constant cryopreservation box microtome to make frozen slices. The prepared frozen sections were dried at room temperature for 10 min, fixed with 4% paraformaldehyde at 4°C for 15 min, and then washed with PBST for use.

To prepare tissue paraffin sections, the tumor nodules were fixed in 10% neutral formalin for 48 h, embedded in paraffin and sliced.

Hematoxylin and eosin (H&E) staining

To detect the nodule cells with H&E staining, a single-cell suspension of tumor nodules was centrifuged onto a slice, fixed with 4% paraformaldehyde at 4°C for 15 min, and stained with Hematoxylin for 30 s and Eosin for 10 s. The slice was observed under a microscope (BX53, Olympus, Tokyo, Japan).

To detect the tissue pathological change with H&E staining, paraffin sections of tumor nodules were stained with hematoxylin for 20 min. After PBS washing, the sections were treated with HCl-Ethanol for 3 s and washed with water for 20 min followed by staining with eosin for 5min. After washing with water for 20 min, the sections were dehydrated with gradient alcohol, precessed transparently with xylene, and sealed for use. The H&E stained sections were observed under microscope (BX53, Olympus, Tokyo, Japan). The necrotic area at central area of nodule tissue section was analyzed by using ImageJ "Color Threshold". In addition, we adjust the precise size by "Saturation" and "Brightness". And then work out the ratio of necrotic area to total area using "Analyze Particles".

Immunofluorescence assay

In immunofluorescence assay, nonspecific cellular immunofluorescence analysis was conducted by staining cells with Evans blue, while specific cellular immunofluorescence analysis was performed by surface staining cells with anti-Ly6G-PE mAb. The cells were then fixed in 4% paraformaldehyde, stained with DAPI, and observed under a fluorescence microscope (BX53, Olympus, Tokyo, Japan) or confocal fluorescence microscopy (FV3000, Olympus, Tokyo, Japan).

In immunofluorescence assay of frozen tumor nodule sections, anti-Ly6G-PE antibody was added dropwise on frozen sections of tumor nodules and incubated at 4°C in dark for 1 h. The sections were observed under a fluorescence microscope (BX53, Olympus, Tokyo, Japan).

Immunohistochemical staining

The paraffin sections were baked at 60°C for 2 h. After deparaffinization and rehydration, antigen retrieval was performed for 20 min. Next, endogenous peroxidase was blocked by 3% H_2O_2 for 10 min. Then, samples were blocked with Blocking Buffer (QuickBlock™ Blocking Buffer for Immunol Staining, Beyotime, China, cat: P0260) for 1 h at room temperature and incubated with 1:200 anti-mouse NK1.1 antibody (anti-mouse NK1.1 Antibody, Biolegend, CAT:108701) overnight at 4°C. In addition, samples were incubated with 1:500 HRP-labeled Goat Anti-mouse IgG (H + L) antibody (Absin, China, cat: abs20001) for 1 h at room temperature. Then, the signal was detected with DAB Horseradish Peroxidase Color Development Kit (Beyotime, China, cat:P0202) for 5–15 min at RT. Hematoxylin counterstain was performed for 30 s at RT. Gradient alcohol dehydration, transparent with xylene, then seal the slides for microscopic observation (BX53, Olympus, Tokyo, Japan). We use ImageJ software to analyze immunohistochemistry results: we first convert the image to 8-bit format, then convert grayscale values to OD values, and set measurement parameters, including "Area, Integrated density, Limit to threshold". At last, we select positive regions and measure their average OD value.

Establishment of *in vitro* experiment system

To trace the fate of tumor cells after trogocytosis of neutrophil, we conducted an *in vitro* experimental system. After GFP-B16 cells were adhered to overnight, neutrophil-rich bone marrow cells (BMC) were added at 30:1 ratio, and co-cultured for 3 h. After the suspended cells (which should contain GFP-B16 cells gnawed by neutrophils) were recovered, the flow cytometry was used to detect GFP⁺Ly6G⁺ cells in part of the suspended cells. The remaining suspended cells were added to the new culture plate and re-cultured for 24 h to determine whether the

remaining tumor cells could survive and grow. For the latter purpose, suspended cells at 0 h were as control. After 24 h, the re-cultured cells in the culture plate were examined under a fluorescence microscope, and GFP$^+$ tumor cells were counted and analyzed.

To prove that trogocytosis can kill tumor cells, B16 cells were inoculated subcutaneously into mice. Tumor nodules were harvested at 24 h of the inoculation, and neutrophil-rich nodule cells were obtained through homogenization as effector cells. GFP-B16 cells were cultured overnight as target cells. The nodule cells were added to the adherent GFP-B16 cells according to the effect to target ratio of 35:1 followed by continually culturing for another 48 h. After that, GFP$^+$ tumor cells were observed under fluorescence microscope. In the experiment system, GFP-B16 cells were used as blank control, and the co-culture system of GFP-B16 cells and mouse peritoneal lavage cells (PLCs) was used as positive control. To prepare neutrophil-rich PLCs, mice were given two intraperitoneal injections of Thioglycollate Medium (TM) at 12 h intervals. At 12 h after the last injection, the mouse abdominal cavity was washed back and forth with PBS to recover the lotion.

To study the effect of tumor cells on neutrophils *in vitro* (Figure S1), bone marrow cells (BMCs) were isolated from the femur and tibia of naive C57BL/6 mice by removing the epiphyses of both ends of bones followed by flushing using 5 mL syringe containing RPMI 1640 medium/ 2% (V/V) fetal bovine serum (FBS). The BMCs were filtered with 300 mesh nylon cloth followed by lysing the erythrocytes in the BMCs with ACK lysis buffer to make the single BMC suspension. To establish a co-culture system *in vitro* with B16 cells, 4×10^5 BMCs were cultured with 1×10^5 GFP-B16 cells in RPMI 1640 medium/10% FBS for 1, 3 and 6 h in a 5% CO_2 humidified incubator at 37°C. BMCs were cultured alone as a control. Then, the suspended cells in the co-culture system were harvested and surface stained with PE-labeled anti-Ly6G mAb (BD Biosciences, NJ, USA, cat: 551461). The stained cells were detected and analyzed by BD-Accuri C6 flow cytometer.

RNA interference assay

For *in vitro* RNA interference (RNAi) assay, *Cxcl2* siRNAs (SIR-93, SIR-131 and SIR-207) or control siRNA (SIR-Ctrl) were used. Firstly, GFP-B16 cells were adherent cultured in RPMI 1640 medium/10%FBS, starved in serum-free medium for 4 h when they reached to 70–80% confluent, and then their medium was replaced with Opti-MEM. The mixture of siRNA/Lipofectamine 2000 was added into the medium of cultured cells at 1/4 ratio followed by incubating for 4 h. After that, the cells were cultured in RPMI 1640 medium/10%FBS for 1 h or 3 h and then collected for isolating the total RNA of the transfected cells with Trizol. The *Cxcl2* mRNA in those transfected cells was detected by RT-qPCR, and its relative expression was represented by $2^{-\Delta\Delta Ct}$. For *in vivo* RNAi assay, *Cxcl2* siRNAs (SIR-93) or control siRNA (SIR-Ctrl) were injected subcutaneously at a dose of 5μg/mouse, respectively, at the same site where GFP-B16 cells were simultaneously inoculated. The *Cxcl2, Cxcl10, Cxcl13, Ccl19* mRNA in tumor nodules 24 h after tumor cell inoculation were detected by RT-qPCR and its relative expression was analyzed with the $2^{-\Delta Ct}$. All siRNAs were synthesized by Haixing Biosciences (Jiangsu, China). The specific sense sequences of siRNAs targeting *Cxcl2* were as follows: SIR-93 5'-CAGUGAACUGCGCUGUCAATT-3'; SIR-131 5'-GGGUUGACUUCAAGAACAUTT-3'; SIR-207 5'-CACUCUCAA GGGCGGUCAATT-3'; SIR-Ctrl 5'-UUCUCCGAACGUGUCACGUTT-3'.

Total RNA isolation and RT-qPCR

Total RNA was isolated from either siRNA transfected GFP-B16 cells or tumor nodules with Trizol (CWBIO, cat: CW0580S). After quantifying the total RNA, the same amount of total RNA was taken from each sample for reverse transcription using cDNA synthesis kit including Oligo dT, 2×ES Reaction Mix and EasyScript®RT/RI Enzyme Mix (TransGen Biotech, Beijing, China, cat: AE301-02). RT-qPCR was performed using two-step SYBR green qPCR assays (PerfectStart® Green qPCR SuperMix, TransGen Biotech, Beijing, China, cat:AQ601) and the *Cxcl2, Cxcl10, Cxcl13, Ccl19* gene was amplified with the specific primers. The data were acquired using the Step One real-time PCR system (Applied Biosystems, Foster City, CA, USA). The PCR procedures were as follows: one cycle at 94°C 30 s followed by 40 cycles at 94°C 5 s and 60°C 31 s. The purpose mRNA levels were analyzed with $2^{-\Delta Ct}$ or $2^{-\Delta\Delta Ct}$ method based on the mRNA levels of Mus *β-actin*. The forward and reverse primers used in this study were as follows: *Cxcl2* 5'-GCGCCCAGACAGAAGTCATA-3' and 5'-CGAGGCACATCAGGTACGAT-3; *β-actin* 5'-TG TGACGTTGACATCCGTAA-3' and 5'-CCACCGATCCACACAGAGTA-3'; *Cxcl10* 5'-GTCCACGTGTTGAGATCATTGC-3' and 5'-CTCTGTGT GGTCCATCCTTGG-3'; *Cxcl13* 5'-ATATGTGTGAATCCTCGTGCCA-3' and 5'-GGGAGTTGAAGACAGACTTTTGC-3'; *Ccl19* 5'-CCTTCAGCC TGCTGGTTCTCT-3' and 5'-AGGCTTTCACGATGTTCCCAG-3'.

QUANTIFICATION AND STATISTICAL ANALYSIS

Statistical analysis was performed using GraphPad Prism 8.0 for Windows (GraphPad Software, San Diego, California, USA), and experimental data were displayed as mean $\pm$ standard deviation. An unpaired t-test was used to compare groups. Survival curves of mice were estimated and compared using the Mantel-Cox test and Gehan-Breslow-Wilcoxon test. And tumor growth curves of mice were estimated and compared using Sidak's multiple comparison test. Differences were considered statistically significant for *p* values <0.05. All experiments were performed at least 2–3 times.